

Tagging of Oil Under Ice - Phase II: Ice Floe Tracking System

Final Report
Contract # E17PC00022

Bureau of Safety and Environmental
Enforcement (BSEE)

June 30, 2019

Prepared for:

Bureau of Safety and Environmental Enforcement (BSEE)
45600 Woodland Road
Sterling, VA 20166-9216

Prepared by:

Ben Schreib,¹ Manuel Sanchez,¹ Stephen Sporik,¹ Sam McClintock,² Ted Hale,² Elizabeth Skinner,² Navid Yazdi,³ Siva Aduri,³ Casey Wallace,³ Mark Hinders⁴

AECOM,¹ Midstream Technology,² Evigia Systems,³ William and Mary⁴

This final report has been reviewed by the Bureau of Safety and Environmental Enforcement (BSEE) and approved for publication. Approval does not signify that the contents necessarily reflect the views and policies of the BSEE nor does mention of the trade names or commercial products constitute endorsement or recommendation for use.

This study was funded by the BSEE, U.S. Department of the Interior, Washington, D.C., under Contract E17PC00022.

June 30, 2019

Point of Contact:

Ben Schreib
Project Manager
T: 410.379.5827
M: 301.305.8170
E: ben.schreib@aecom.com

AECOM
430 National Business Parkway
Annapolis Junction, MD 20701
aecom.com

Table of Contents

1.	Executive Summary	1
2.	Phase I Summary	3
	2.1 System Architecture and Components	3
	2.2 System Testing	4
	2.3 Modeling and Simulation	4
	2.4 Navy Ice Exercises	7
	2.5 Utqiagvik (Barrow), Alaska	7
3.	Phase II: System Components	8
	3.1 Modeling and Simulation Supporting Phase II Designs	9
	3.2 Second Generation Untethered UWID	15
	3.3 Second Generation LDGRIDSAT	16
	3.4 Remotely Operated Vehicle	17
	3.5 Cloud Infrastructure and GIS Web Application	18
	3.6 Software Tools Employed	18
	Cloud-Based Data Servers	19
	Phase II Updates	20
4.	Utqiagvik Testing and Analysis	20
	4.1 Laboratory and Pool	21
	4.2 Problems Encountered during Testing	21
	4.3 Location, Setup Equipment and Configuration	22
	4.4 Data Collection	24
	4.5 Analysis	26
5.	Cass Lake, MN, Testing and Analysis	32
	5.1 Location, Setup Equipment and Configuration	32
	5.2 Data Collection	33
	5.3 Analysis	33
6.	Commercialization Plans	37
7.	Conclusion	37
8.	References	38
	Appendix A – LDGRIDSAT Tag Operations and User Guide	39
	LDGRIDSAT	39
	Setup	39
	Startup	39
	Configuration	40
	Appendix B – Mapping User Interface User Guide	42

Figures

Figure 1: Ice Floe Tracking System concept of operations.....	2
Figure 2: Illustration of the IFTS primary components and architecture.....	3
Figure 3: First generation UWID prototype.....	3
Figure 4: First generation LDGRIDSAT aerially deployed (left) and surface-deployed (right) prototypes.....	4
Figure 5: Simulated longitudinal wave modes and shear waves in 1-meter-thick ice.....	5
Figure 6: Geophysical Research Facility (GRF) sea ice tank at CRREL.....	6
Figure 7: CRREL GRF signal capture, filtering and detection.....	6
Figure 8: Navy ICEX LDGRIDSAT tag aerial deployment testing.....	7
Figure 9: IFTS demonstration off the coast of Utqiagvik, AK.....	8
Figure 10: Second generation UWID design.....	9
Figure 11: Simulation of modeled space.....	10
Figure 12: Signal emitted by simulated transducer.....	10
Figure 13: Simulation output format.....	11
Figure 14: Simulation output.....	12
Figure 15: Critical angle vs. max angle phase space.....	13
Figure 16: Phase plot.....	14
Figure 17: External and internal views of the second generation UWID.....	15
Figure 18: LDGRIDSAT tag deployed.....	16
Figure 19: Internal pictures of first and second generation LDGRIDSAT tags.....	17
Figure 20: Deep Trekker DTX2 remotely operated vehicle.....	17
Figure 21: Cloud infrastructure schematic diagram.....	18
Figure 22: Deploying and test driving the ROV at a W&M pool using cold weather gloves.....	21
Figure 23: Setting up the test site on ice floes off the coast of Alaska.....	22
Figure 24: Deployment of the tethered UWID under the ice floe.....	23
Figure 25: A tethered accelerometer and LDGRIDSAT tag.....	23
Figure 26: Deployment of the UWID using an ROV.....	24
Figure 27: Unfiltered topside recording of the signal from the untethered UWID.....	26
Figure 28: Bandpass filter isolates 1 kHz signal.....	27
Figure 29: Cross correlation results.....	28
Figure 30: Dynamic wavelet fingerprint and kernel used for 2D analysis.....	29
Figure 31: Denoised signal, convolution using 10 seconds of UWID pulse as the kernel, and convolution using 2-second pulses as the kernel.....	30
Figure 32: LDGRIDSAT tag gateway report from the test site off the coast of northern Alaska.....	31
Figure 33: Area of Cass Lake where IFTS testing was conducted.....	32
Figure 34: Test site and direction of LDGRIDSAT and accelerometer placement.....	33
Figure 35: Detection of UWID signal at 1 kilometer.....	36

Tables

Table 1: UWID Settings, Test Data Collection, and Detection Determination.....	25
Table 2: LDGRIDSAT Report.....	31
Table 3: UWID Test Settings and Detection Confidence.....	34
Table 4: Types of UWID Tests Performed.....	35

1. Executive Summary

The Ice Floe Tracking System (IFTS) was developed under the Department of Interior Bureau of Safety and Environmental Enforcement (BSEE) project known as “Tagging of Oil under Ice for Future Recovery.” This final report provides a summary of Phase I and describes the findings and data for Phase II of the Tagging of Oil under Ice for Future Recovery project.

AECOM, in collaboration with Midstream Technology, Evigia Systems, and the College of William and Mary (W&M) started Phase I of the project in 2014, and successfully delivered a two-part technology for autonomous and long-term tracking of ice floes in the Arctic. These two parts consisted of:

- 1) A surface tag: the Lamb-wave Detection Geo-Referencing Identification Satellite (LDGRIDSAT), a sensor and communication device about the size of a 1-liter bottle that housed an Iridium satellite modem, computer, WiFi, GPS and accelerometer that could be deployed manually with an ice anchor, or aurally from any height, and not only track the ice floe, but also “listen” for the guided/Lamb/Rayleigh waves generated by a subsurface tag, and
- 2) A subsurface tag: the Underwater Identification (UWID), a large 1-foot-diameter underwater device that housed a computer and transducer plate with batteries that could be deployed by a submersible, in turn generating acoustic pulses directed into the ice for detection and location by the LDGRIDSAT tags.

Phase II was established to advance new IFTS designs and test their performance in real-world conditions. These improvements were completed and tested to accomplish the project’s performance objectives:

- 1) Objective 1 was met through updates to the LDGRIDSAT accelerometer, internal mechanical mounting and enclosures for both manual and aerial deployment. These changes introduced accelerometers with higher sampling rates, improved the survivability of the second-generation LDGRIDSAT tag to aerial drops, and incrementally increased the performance and biodegradable characteristics of the tag enclosure and backplane.
- 2) Objective 2 was met through a completely new second-generation UWID design to accommodate a new variable-frequency transducer, battery pack and improved enclosure with mounting points for deployment by an underwater vehicle. The new UWID design increased the power and time-on-station and reduced the number of moving parts and overall complexity from the original design. The UWID also had a lower profile to reduce drag when being deployed by an underwater unmanned autonomous vehicle (UAV).
- 3) Objective 3 was met by testing the second-generation LDGRIDSAT tags and second-generation UWID tag in an Arctic environment. We were able to show a full system test including satellite communication and display on the geographic information system (GIS) interface. A detection range of 1 kilometer was also accomplished.

In April 2018 the AECOM team traveled to Utqiagvik (Barrow), Alaska, to test the Phase II components on Arctic ice floes. However, almost all of the test equipment, including the underwater remotely operated vehicle (ROV), was damaged during shipping. The team was able to repair some of the equipment and conducted an underwater deployment of the UWID using the ROV and tested the IFTS despite inclement weather and high winds. Testing ended when ice floe melting and encroaching water of the Beaufort Sea restricted tests for long-range detections (100 m to 1000 m) of the UWID by the LDGRIDSAT tag.

Because of the paucity of long-range testing data, the team conducted an additional series of tests in February 2019 on the frozen surface of Cass Lake near Bemidji, Minnesota. The team used two different UWID tags together with LDGRIDSAT tags and tethered high-sample-rate accelerometers, collecting over

500 data sets at distances of 10 m to 1200 m. These tests validated the IFTS technology and demonstrated that the UWID tags' guided waves could be detected at distances to 1 kilometer.

The original concept of the IFTS was envisioned as components working independently or together to provide situational awareness by tracking ice floes identified to contain entrapped oil for future recovery. Figure 1 illustrates the concept of operations from one potential oil spill vector with a variety of methods for deploying aerial and hand-deployed LDGRIDSAT tags. The UWID tags are deployed underneath the ice floes to communicate their location to the topside LDGRIDSAT tags, which in turn communicate through a global satellite network back to the GIS user interface for stakeholders to track daily movements of ice floes.

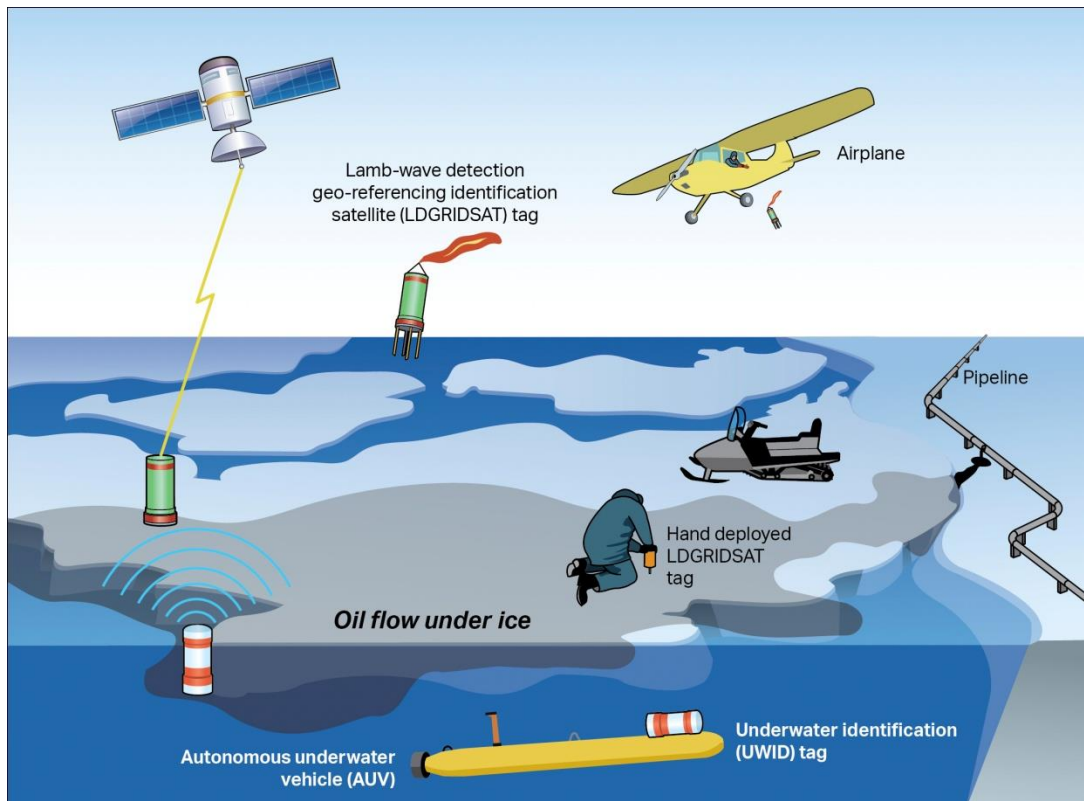


Figure 1: Ice Floe Tracking System concept of operations

These tests demonstrated that the IFTS works well for tracking ice floes. The LDGRIDSAT tag can be deployed by hand or by air, can transmit for months at a time to track any one ice floe section, and can be modified to accept different sensor packages. Logistically, the LDGRIDSAT tags have components that are easily found or produced, and are a compact size that can be transported and stored for years without impacting functionality. The use of the Iridium polar-orbiting network means that the tag can communicate from anywhere in the world, so the tag would also be useful to other countries and companies operating in extreme latitudes. The LDGRIDSAT can be produced commercially without extensive modification and can be in the hands of response teams within months of placing an order.

The UWID works, but it is not as easy to produce as the LDGRIDSAT tag. The UWID requires a minimum 8-inch transducer plate to generate the 1 to 2 kHz signals, and the transducer alone costs more than several LDGRIDSAT tags. The UWID requires a fairly substantive battery pack to project the power and duration for long-range detection. These requirements lead to a heavy, expensive underwater beacon—up to 50 pounds for a device that may be rarely deployed. In addition, for the LDGRIDSAT tag to reach detection ranges of 1 kilometer, the UWID needs to broadcast maximum power over several minutes, reducing its operational period to only several weeks.

2. Phase I Summary

The AECOM team derived and analyzed system performance requirements based on the objectives established by BSEE to develop LDGRIDSAT tags and UWID tags and to test these in an arctic environment as detailed in reference [2]. We developed trade studies and an analysis of alternatives prior to detailed designs of each component, device and software system that comprises the IFTS. Our team modeled and simulated operational environments, fabricated and unit tested each piece of the system in realistic environments and then deployed and demonstrated the IFTS on an ice floe in the Arctic off the coast of Utqiagvik, AK.

2.1 System Architecture and Components

Figure 2 shows the basic architecture of the IFTS and interfaces between devices.

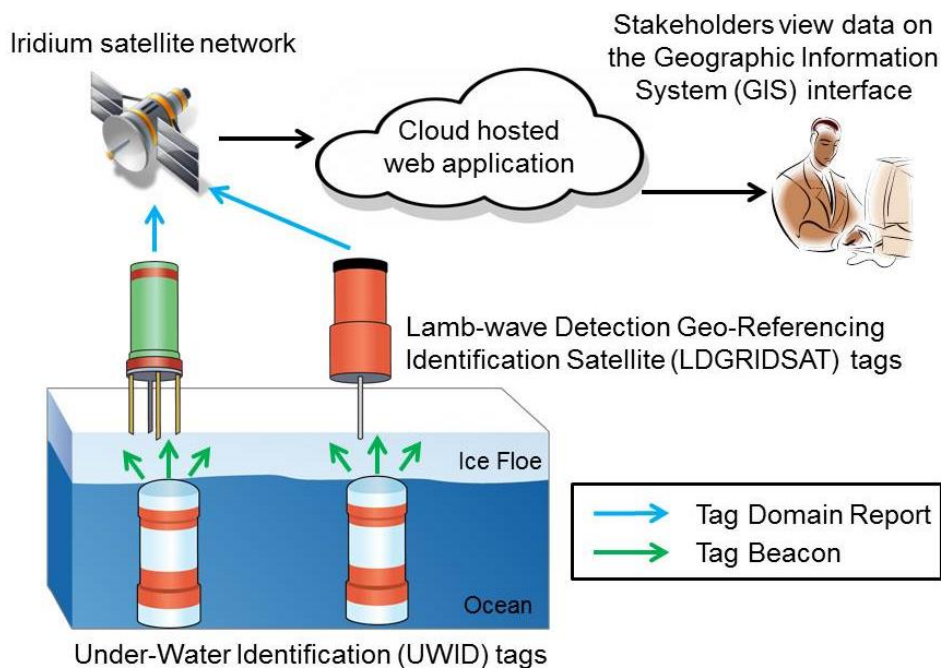


Figure 2: Illustration of the IFTS primary components and architecture

The primary components and functionality of the deployed system are:

Underwater Identification (UWID) – The UWID tag is equipped with an acoustic transducer that projects sound at a critical angle to the ice creating Lamb waves and Rayleigh waves, collectively referred to as guided waves. The UWID tag is deployed underneath the ice with sufficient buoyancy to float up through sea water and oil to the bottom surface of the ice. The UWID guided wave acts as the tag beacon signal to be detected by the surface deployed LDGRIDSAT tag. The communication has no overlying protocol; it is a simple detect mode by the LDGRIDSAT of the UWID acoustic guided wave. The detection is only one bit, 0 for no signal, and 1 for a signal.



Figure 3: First generation UWID prototype

The original UWID design was spherical (Figure 3) with the core components moving inside the sphere to correctly orient the transducer to project into the ice floe. Because of the complexity of the design, number of moving parts, and limited payload space for batteries, it led to the Phase II design shown in Section 3.2.



Figure 4: First generation LDGRIDSAT aerially deployed (left) and surface-deployed (right) prototypes

Lamb-wave Detection Geo-Referencing Identification Satellite (LDGRIDSAT) – The LDGRIDSAT tag can be used by itself to mark a location, or it can be combined with an onboard guided wave detector that can locate one or more UWID tags placed under the ice. The UWID tag beacons are aggregated along with the LDGRIDSAT tag message and sent from the LDGRIDSAT tag to the server over the Iridium satellite network to the cloud infrastructure for interpretation and further processing for final display on the mapping user interface. The AECOM team felt that both an aerially deployed and surface-deployed variant of the LDGRIDSAT tag would be necessary to meet the operational requirements of response teams in the Arctic. These two variants of the LDGRIDSAT tag are shown in Figure 4.

Aerial Drop LDGRIDSAT Tag – The aerial drop tag is designed to impact solid ice from an altitude exceeding 100 m and stick upright with the metal spikes (tines) in contact with the ice. The aerial tag uses a plastic streamer to maintain vertical orientation at impact. The accelerometer of the tag is mounted to a solid base to which all the tines connect. The final configuration uses copper tines. These copper tines collapse on impact (like the front of a car in a collision), penetrating the loose ice and snow on the ice floe surface without bouncing and lodging the tag firmly in the ice.

Ice Anchor LDGRIDSAT Tag – This variant is meant to be manually deployed by screwing the tag into the ice. The ice anchor is hollow, and the accelerometer is placed inside the ice anchor. The first

generation uses a stainless steel ice anchor, but subsequent designs can use a hard, biodegradable plastic anchor tipped with stainless steel.

Cloud Infrastructure and User Interface – This backend system includes the satellite network and internet routing needed for the LDGRIDSAT tag to communicate to the cloud-based data servers. The server and database interact with the GIS software that incorporates a user interface for extracting and displaying the actionable information to stakeholders.

2.2 System Testing

At the beginning of the design phase, our team completed a trade study and assessment of various commercial off-the-shelf technologies and available companies to guide the design and fabrication for deployment of the IFTS for tracking oil under ice floes in Arctic marine environments. We developed models and ran simulations of various environments for acoustic wave propagation, unit tested the IFTS component devices, tested parts of the system at the Cold Regions Research and Engineering Laboratory (CRREL), and conducted Navy Ice Exercises (ICEX) and a full system demonstration in Utqiagvik, AK.

2.3 Modeling and Simulation

A key part of the design process was to explore options via simulation. We analyzed the Group Velocity Dispersion Curve for sea ice and determined that most guided wave modes will arrive at the topside LDGRIDSAT tag at approximately the same time to detect any guided wave. William and Mary used a variety of tools including Visco-Elastic Finite Integration Wave Solver, Geoacoustic_TDFD and SoundSim to model and simulate acoustic wave propagation and scattering in sea ice between layers of sea water

and air. We showed that a change in thickness of the ice does not significantly change the guided wave propagation and, as captured in Figure 5, that waves interacting with a crack up to about half the depth of the ice continue to propagate.

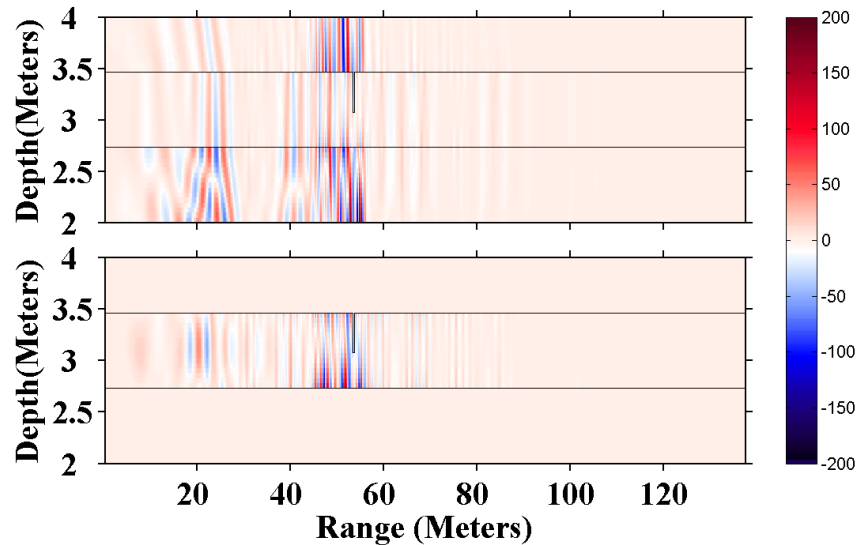


Figure 5: Simulated longitudinal wave modes and shear waves in 1-meter-thick ice

Over 300 sound files were collected as part of this testing at CRREL’s Geophysical Research Facility (GRF) with simulated sea ice (Figure 6). The relatively small surface area of the ice (1320 ft²) combined with the GRF’s containment walls, upward-sloping edge of the pool at the far end, and a shallow depth reflected the UWID tag’s sound from multiple surfaces. The frequency of the UWID, combined with the thickness of the ice, generated a sound front of multiple guided waves that had approximately the same velocity. The original signal and guided wave products were detected, but the instrument could not detect signal degradation beyond a few meters because of the reflections and wave velocity. This behavior negated a detection distance extrapolation beyond the confines of the test surface. All the accelerometers were able to detect the signal both directly near the source and through the guided wave products of the signal through the ice. The LDGRIDSAT tags that were sampling at 3.2 kHz detected no degradation of signal, again because of the constant reflection of sound. Post-CRREL analysis helped the team to construct pre-processing filters that were used in LDGRIDSAT tags for real-time detection of acoustic signals for the Utqiagvik, AK testing.

Figure 7 shows one of these sound files and the process from raw data collection before filtering, the application of a Fast Fourier Transform (FFT) to the frequency domain and filtering, revealing the pulsed signal hiding in the noise.

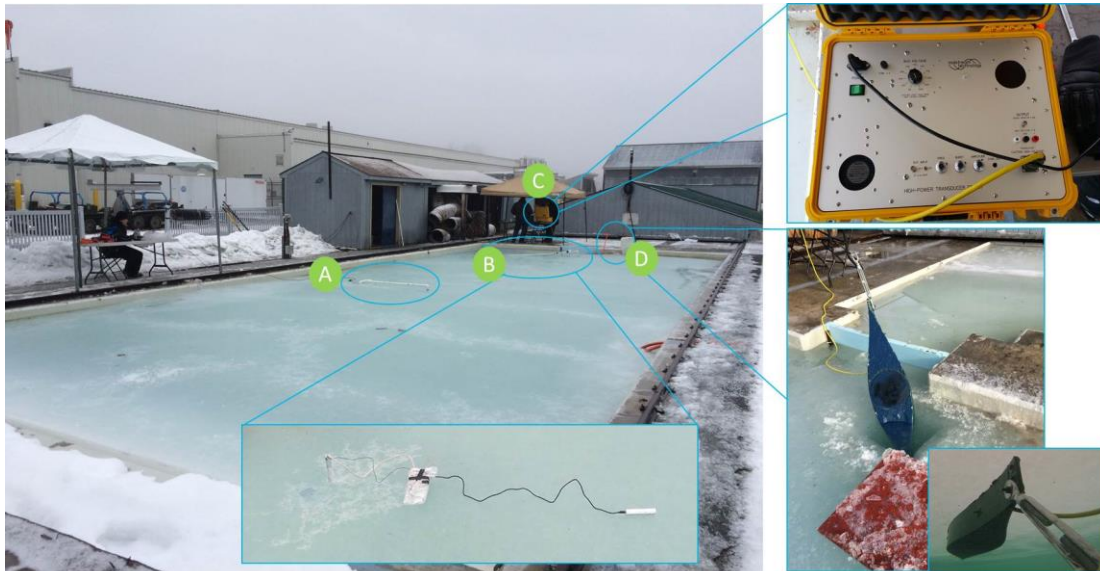


Figure 6: Geophysical Research Facility (GRF) sea ice tank at CRREL

- A. Raw data collection from an accelerometer sampling at 44.1 kHz at fixed intervals along the sea ice
- B. Battery-powered single board computer with accelerometer embedded in an ice screw to mimic an LDGRIDSAT detector
- C. Transducer driver and signal generator for the tethered test version of the UWID
- D. Tethered test version of the UWID tag shown being inserted and positioned underneath the ice

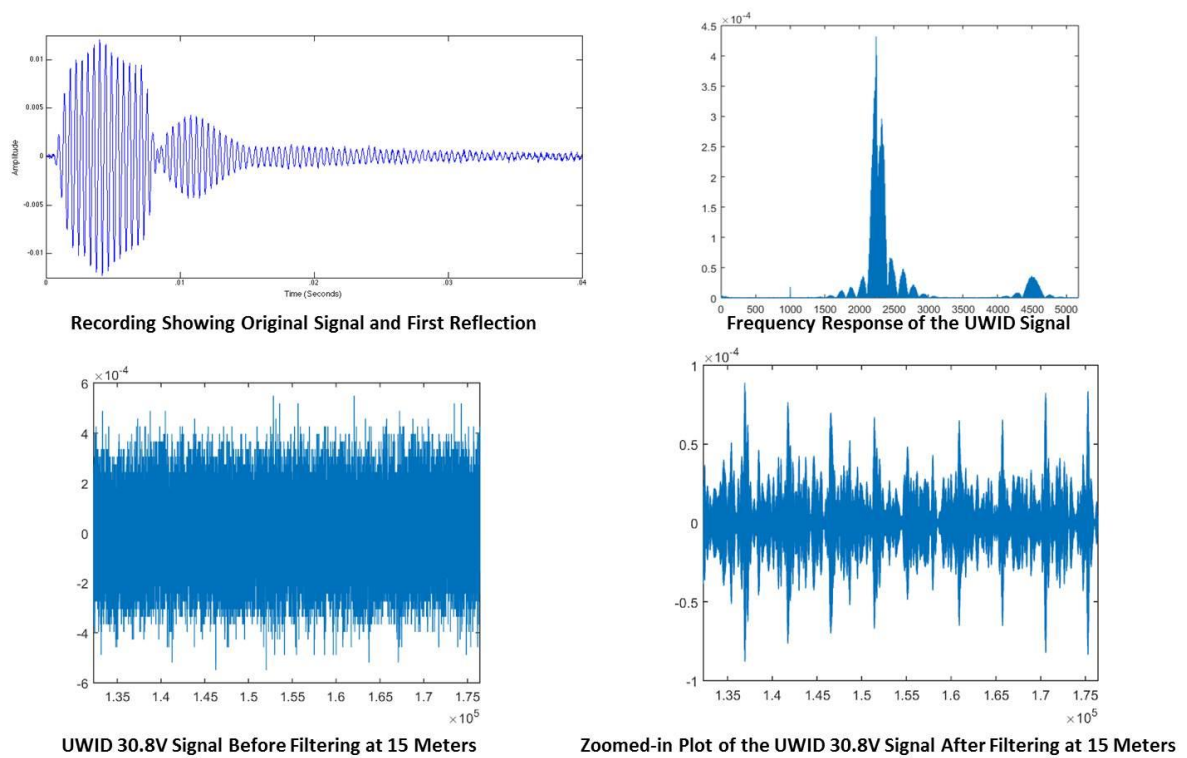


Figure 7: CRREL GRF signal capture, filtering and detection

2.4 Navy Ice Exercises

The purpose of the 2016 ICEX testing was to demonstrate the efficacy and survivability of aerially and manually deployed surface LDGRIDSAT tags. ICEX testing involved the aerial deployment of four LDGRIDSAT tags. All four housings and payloads survived the aerial drop, and the two tags with thinner (1/16-inch) copper spikes imbedded properly in the ice floe. The left photo of Figure 8 shows one of the tags being tossed out of a helicopter from 150 meters above the ice. The middle photo shows the tag properly oriented and embedded through the snow and making contact with ice. The photo on the right of Figure 8 shows the same tag after being retrieved.



Figure 8: Navy ICEX LDGRIDSAT tag aerial deployment testing

2.5 Utqiaġvik (Barrow), Alaska

The primary goal of the Utqiaġvik testing was to demonstrate the survivability of the ice anchor surface tag and determine whether acoustic signals generated under the ice floe by the UWID tag could be detected by a surface tag above the ice floe and then relayed through a satellite network to a cloud infrastructure for display on a user interface.

Figure 9 is a vignette of our test setup and demonstration of the IFTS off the coast of Utqiaġvik, AK. The UWID was deployed underneath the ice and projected a series of acoustic shots into the bottom surface of the ice, which were detected by the surface LDGRIDSAT tag; this message was then relayed through the satellite network to the cloud infrastructure and displayed on the GIS user interface web application.



Figure 9: IFTS demonstration off the coast of Utqiagvik, AK

All test equipment worked as expected, the UWID tag floated correctly to the bottom surface of the ice, and the accelerometers in use picked up the immediate high-voltage signals. The signal the UWID transmitted was intentionally very narrow-banded to allow the received signal to be filtered out of the noise, but it also reduced the amount of data to be analyzed. Combined with a narrow sound front and no reflections, it appears that the accelerometer sampling rate of 3.2 kHz was too slow to gather the amount of data needed to filter out the sound from ambient noise as the sensors got farther from the UWID tag. We used the pre-processing filters in Utqiagvik, AK, and were able to detect the signal at ranges within 10 meters, but not beyond. The LDGRIDSAT tags did report receiving a signal at other distances, but not enough times to conclude positive responses, or rule out false positives, of the system as a whole.

The Utqiagvik test showed that the LDGRIDSAT tag can be deployed manually by use of an ice anchor at the base of the tag and that the LDGRIDSAT tag can operate for extended periods in the Arctic environment. LDGRIDSAT tag 759510 was able to continuously report for 57 days. The UWID tag was a success in that the LDGRIDSAT tag detected the UWID acoustic signature out to 10 m. However, the LDGRIDSAT tag could not detect the UWID tag at larger distances.

3. Phase II: System Components

This section describes the design elements, modifications, and component integration to the baseline Phase I design for the UWID, LDGRIDSAT, ROV integration, and cloud infrastructure and GIS web application.

3.1 Modeling and Simulation Supporting Phase II Designs

Modeling Summary: Because our team felt the initial UWID tag design was inadequate because it required moving parts in a spherical design, a design that also limited space for batteries, the UWID went through another design phase. The second generation design resulted in a cylinder with curved cap ends. Once deployed, the UWID would float in a vertical orientation until it hit the ice floe with the transducer oriented correctly for broadcasting the acoustic signal into the ice. As part of this effort, the W&M and Midstream contingents of the team modeled various characteristics of the new UWID design. The results of this modeling, described below, allowed our team to design reflecting surfaces above and below the acoustic transducer inside the UWID. These surfaces optimized the amount of signal reflected into the ice floe each time the transducer was activated.

The Cylindrical Acoustic Finite Integration Technique (CAFIT) was developed by Peiffer et al. as an extension of an acoustic finite integration technique in the cylindrical coordinate system [1]. By discretizing in the cylindrical coordinate system, they found that they could simulate three-dimensional (3D) problems in a two-dimensional (2D) space assuming the solutions were axisymmetric. For this reason, CAFIT is sometimes referred to as a 2.5-dimension simulation. This efficient simulation method was used to design the size and shape of the reflectors inside the chamber of the UWID tag, as shown on Figure 10.

In second generation design, the transducer is the SX105 bender transducer from Sensor Technologies. It is 8 inches in diameter and 2.2 inches thick, has a variable frequency range of 400 Hz to 2.5 kHz and is omnidirectional below 2 kHz. It sits in a chamber filled with an acoustic couplant and reflectors above and below to reflect the emitted signals up toward the ice at the critical angle of about 26 degrees. Based on the simulations, the top reflector was chosen to have a half angle of 40 to 45 degrees, and the bottom reflector was chosen to be flat. Below this chamber is an air-filled chamber that holds the electronics and batteries necessary to power the transducer. The batteries also act as ballast, and additional ballast can be added at the bottom to balance the UWID for vertical operation and to float up and into the ice floe.

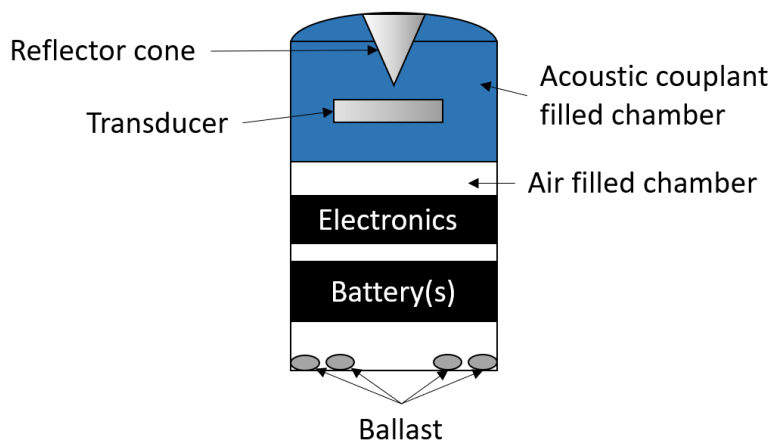


Figure 10: Second generation UWID design

To quantify the propagation angle of the acoustic waves in the simulations, the energy flux was used [3]. Energy flux was chosen over other measures, such as the Poynting vector [4, 5, 6]. The energy flux is measured by multiplying the pressure field by the velocity field and gives a vector pointing in the direction of propagation with units of energy. The other benefit of using it is that by summing the energy flux over a defined amount of time we get the time averaged energy in that area, which is a useful metric when comparing different simulations.

The UWID tag was designed to survive in the harsh, under-ice environment in the Arctic. Beta polypropylene (bpp) piping with a diameter of 355 cm was used to enclose the components because it is durable and has similar acoustic impedance to water. The upper chamber was filled with an acoustic couplant that has similar acoustic properties to cold Arctic water. Reflectors above and below the Sensor Technologies SX105 Bender Transducer are intended to reflect the omnidirectional signal up toward the critical angle for a water-ice interface, which is about 26 degrees. The notional design of the UWID tag, as seen in Figure 10, is a pill shaped tag with acoustic couplant in a chamber at the top of the tag. The transducer is mounted inside with a reflecting cone above it to redirect the omnidirectional signal toward the critical angle for ice, thus maximizing the acoustic signal that is transmitted up into the ice as laterally spreading guided wave modes. Below the transducer, the interface with the air-filled chamber reflects the signal upward due to the impedance mismatch between air and water. The CAFIT simulations allowed us to optimize the shape of both the reflectors above and below the transducer to maximize the acoustic energy sent into the ice.

The simulation space defines a half space that is 0.3 m along the z axis and 0.5 m along the r axis. Because the solutions are axisymmetric, this space is reflected across the z axis to give a 0.3 m by 1 m simulation space as shown in Figure 11. A color plot of the density inside the simulation space shows how the area is mapped. The blue represents water, with a density of 1000 kg/m^3 . The light gray cones at the top and bottom of the simulation space represent air-filled reflectors with a density of 1.225 kg/m^3 . The gray rectangle represents the transducer, which is modeled as a hard acoustic scatterer. The two black lines represent the edges of the bpp piping holding the UWID tag. Data were collected along the top boundary of the simulation space, represented by the red line.

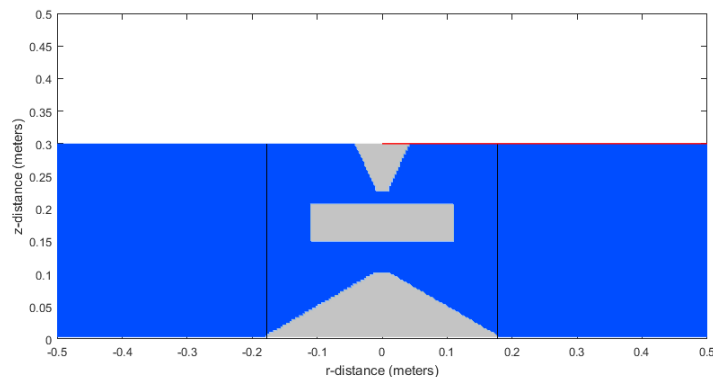


Figure 11: Simulation of modeled space

The transducer has a radius of 0.11 m and a thickness of 0.056 m. In the simulation, it was considered to be a hard scatterer. For visualizations, such as that shown in Figure 12, the density and speed of sound are both defined to be 0.1 in their respective units.

The signal emitted from the transducer shown in Figure 12 was created by adding the defined tone burst, with unit amplitude, to each spatial step on the surface of the rectangle, which defines the transducer. In a sequence of simulations, the height of the conical reflectors can be systematically varied along with the side angle and the width of the tip. This figure shows a 6 kHz sine wave tone burst signal with unit amplitude.

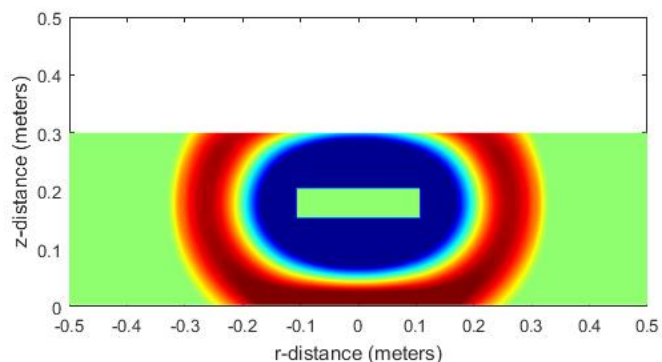


Figure 12: Signal emitted by simulated transducer

The locations of the tips of the conical

reflectors, referred to as top boundary and bottom boundary, are defined by their locations in space relative to the bottom of the simulation space. For numerical stability, the tips of the cones must be at least two spatial steps. The pipe enclosing the chamber has a radius of 0.1775 m, so the reflector cones cannot go past this point in the r direction. Furthermore, since the bpp piping has similar acoustic impedance to water and is thin compared to the wavelength of the acoustic signal, it is assumed to be acoustically transparent in the simulation.

Pressure and both r and z components of the energy flux vector were recorded in time, along the top of the simulation space from the central axis all the way to the right edge, illustrated by the red line at the top of the simulation space in Figure 11. That data were used to output several values to determine the power and the angle of incidence at different points.

Figure 13 shows the outputs for one simulation. In this case there were two conical reflectors, one above the transducer and one below, with half angles of 30 and 15 degrees, respectively. The lines on either side of the transducer represent the walls of the bpp piping. The plot on the top of Figure 13 shows the average angle of incidence as a function of r location. The sharp drop around $r = 0.05$ is a numerical artifact from the cone and can be neglected. In the bottom right plot, the time averaged power at each r location along the top was calculated. The plot on the bottom left was created by finding the maximum squared amplitude at each location along the top of the simulation space. This was then plotted against the average propagation angle at that location, giving the angle of incidence of the most powerful wave.

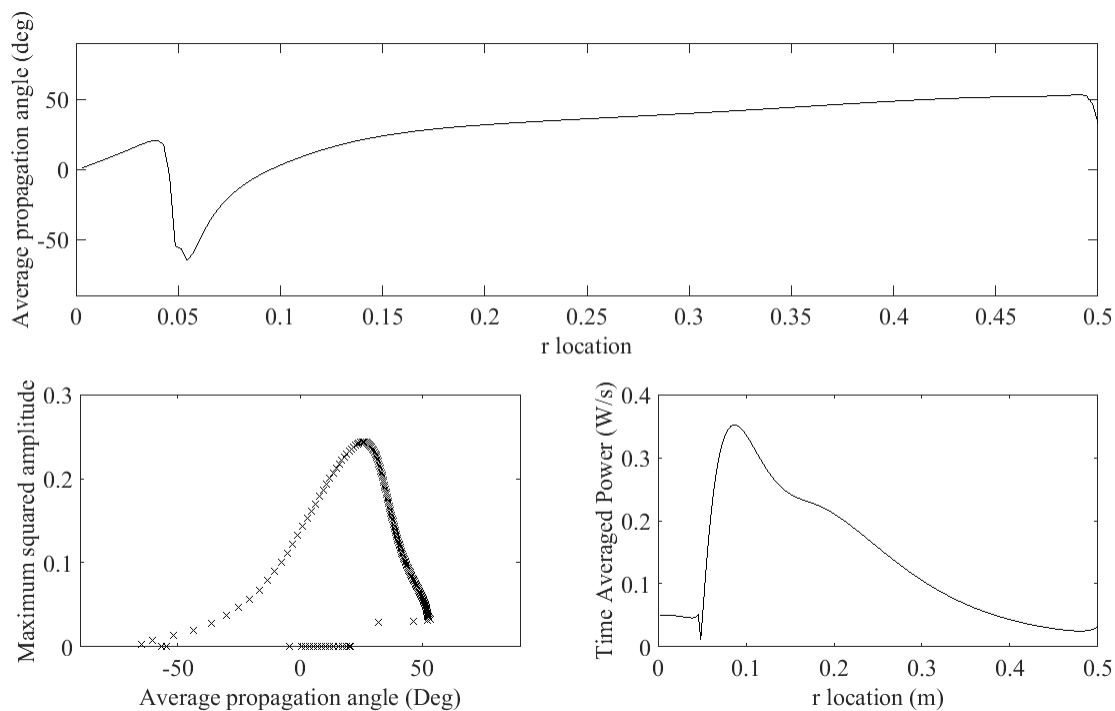


Figure 13: Simulation output format

In order to maximize the total power incident at the ice interface at the critical angle, the team had to compare hundreds or even thousands of simulation results. Figure 14 shows a comparison of these simulations.

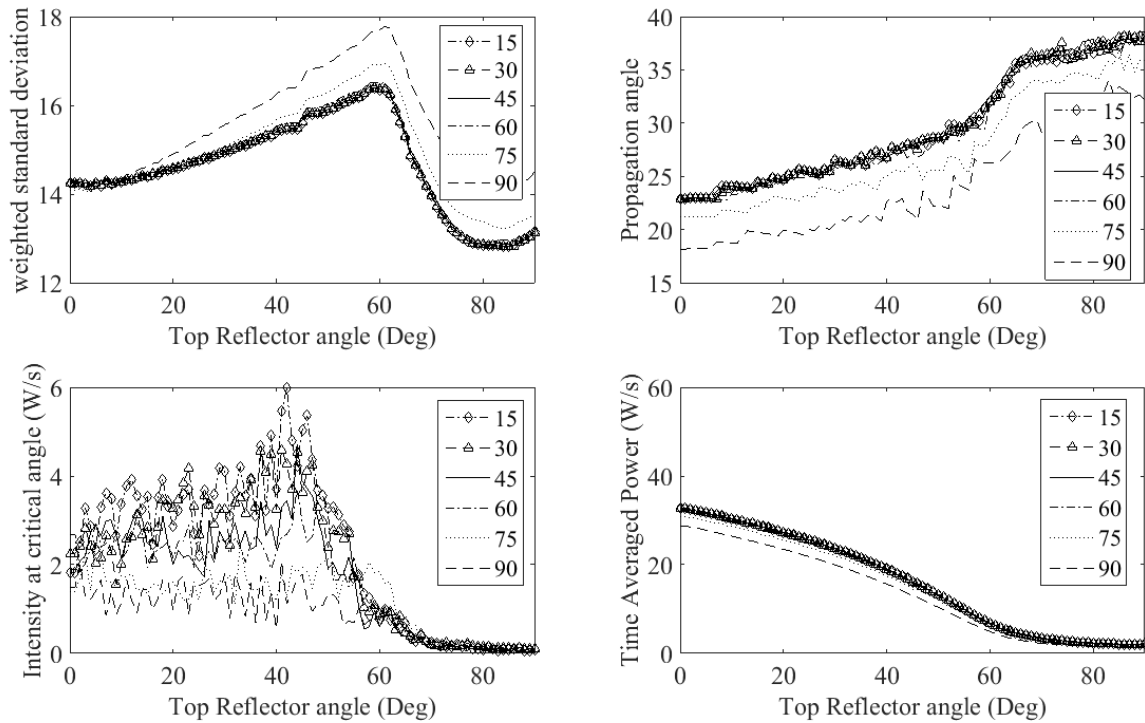


Figure 14: Simulation output

There are four sub-plots for the four different output metrics obtained from a single simulation. The output values plotted are:

- Spread
- Angle of incidence of the wave front with the largest squared amplitude
- Power incident at the critical angle
- Total power at the top of the simulation space

The spread is the weighted standard deviation of the average angle of incidence in space, using the maximum squared amplitude corresponding to each angle as its weight. This gives a measure of how focused the energy is at some angle of incidence such that a higher spread value corresponds to less focus. The angle of incidence of the largest squared amplitude waveform gives the max angle. This max angle is the peak in the bottom left plot of Figure 14 and is the focus angle from the spread value. The last two values are time averaged power values. The first value is the time averaged power of waves incident at the critical angle. This finds every point in time and space where the incident angle was about 26 degrees and adds them together to find the total power at the critical angle. The second value, power, gives the total power incident at the ice interface. This was calculated by integrating the bottom right plot in Figure 14 through space.

Each of these values gives specific information about individual simulations that can be compared to hundreds of other simulations graphically, as demonstrated in Figure 14. In this trial, the angle of the top cone was varied from 0 to 90 degrees in steps of one, while the angle of the bottom cone was varied from 10 to 90 degrees in steps of 15. Each individual line in the plots represents a different bottom cone angle. The x axis of each plot shows how each value changes as the top reflector angle increases. In this example, the bottom cone tip is located 0.07 m from the bottom of the simulation space, and the tip of the top cone is located 0.23 m from the bottom.

Every simulation with different boundary locations produced a result generally resembling those in Figure 14. In each of these plots, the combination of reflectors that resulted in a 26 degree propagation angle determined in the top right plot, and in the highest total power determined from the bottom right plot, was recorded, and so was the combination that resulted in the highest values of critical angle power in the bottom left plot. Each of these scenarios were then run individually to obtain outputs similar to those in Figure 13, allowing them to be compared in more detail.

To compare the selected reflector configurations, phase space plots were created based on these outputs. Figure 15 shows the critical angle vs. max angle phase space. The horizontal axis represents the difference from the critical angle of 26 degrees, with the y-intercept being a max angle value of exactly 26 degrees and positive values along the x axis representing a max angle larger than 26 degrees. The vertical axis is the critical angle power value, which gave the total power of wave fronts incident at the critical angle. The red point shows an optimal configuration with a large critical angle power value directed exactly at 26 degrees. The closest point to this value is point number 15. The cluster farthest from the vertical axis represents the simulation runs that did not have a top reflecting cone. While these configurations had a high critical angle power, they were not focused on the critical angle, so they appear very far away in this phase space.

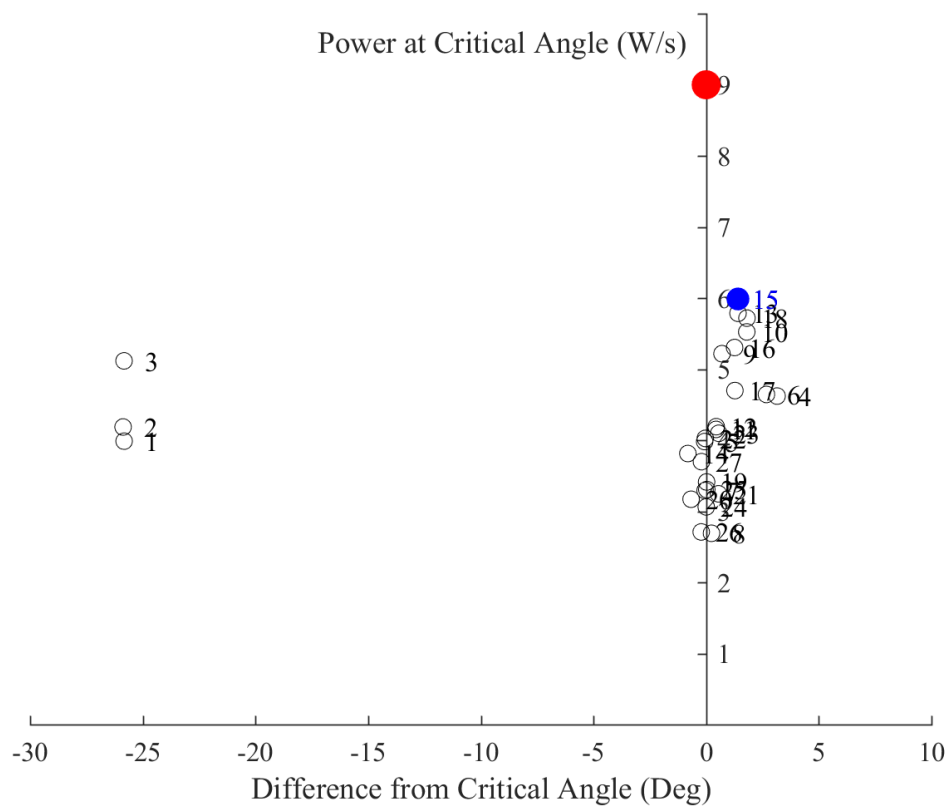


Figure 15: Critical angle vs. max angle phase space

However, in Figure 16 this cluster is much closer to what an optimal configuration might look like. Figure 16 shows the critical angle power and total power phase space where the critical angle power is on the horizontal axis and the total power is on the vertical. The optimal configuration is shown, again, by the red circle in the top right corner. It represents both high total power and a high critical angle power. In this phase space, data point 3 seems to be the closest to the optimal scenario. The bottom cluster, which corresponds to the cluster on the vertical axis in Figure 15 is farther away from this point based on the

total power; however, much of this cluster is closer along the x-axis. Within this cluster, the general trend seems to show that as the total power decreases, the critical angle power increases. Any power that is not at the critical angle is wasted because it will tend to reflect off the ice or induce sub-optimal Lamb wave modes.

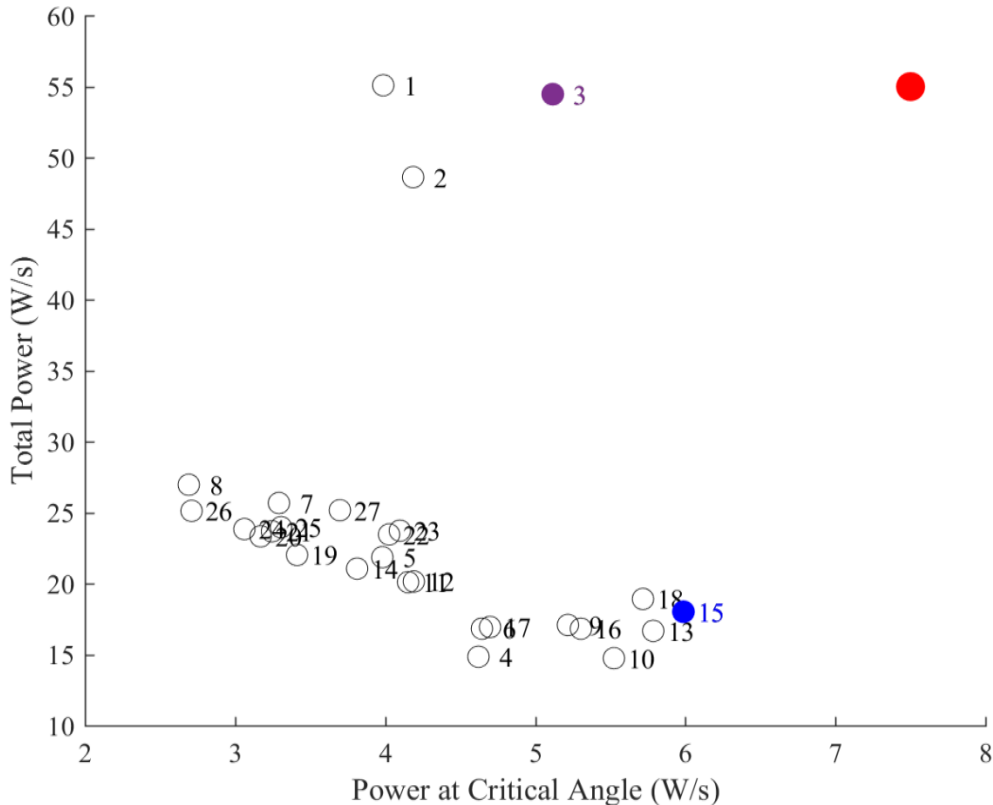


Figure 16: Phase plot

In selecting the best configuration, both Figures 15 and 16 were considered. It is important for the reflectors to focus the signal at an angle of 26 degrees because this leads to much more energy focused around 26 degrees, not just at exactly 26 degrees. This is important because ice varies in thickness throughout the Arctic, so for practical implementation there needs to be a range of incident angles around 26 degrees with non-negligible power. This eliminates configurations that do not utilize top reflector cones. Configuration 15 gives us this focus around the critical angle, as well as a relatively large overall power.

Through these simulations, it was shown that the precise angle of the bottom cone reflector did not make a significant difference in the total power until the angle exceeded 60 degrees. For the critical angle power, the angle of the bottom cone had a non-negligible effect on the results. Generally, 15 to 30 degree reflectors were similar, but angles larger than this dropped the critical angle power significantly. The location of the tip of the bottom cone had a much greater effect on the results. The farther it was from the transducer, the more power was incident on the ice. Because the angle of the bottom reflector was not as important as the distance from the transducer's bottom surface, it was chosen to be flat for buoyancy purposes.

Generally, moving the top cone closer to the transducer gave better results; however, if the cone was too close, more energy was lost inside the cone. Thus, the simulations with the top cone at 0.23 m in the simulation space tended to give the best results. The angle of the top cone changed the behavior significantly. The larger the angle of the sides, the lower the overall power became, but the critical angle

power seemed to increase until the angle hit 60 degrees. This caused a sharp drop in critical angle power and total power. When the top cone was at 0.23 m in the simulation space, a side angle of about 40 to 45 degrees led to high critical angle power such as in elements 13, 15, and 18 in the phase space plots.

3.2 Second Generation Untethered UWID

As discussed earlier, the first generation UWID was too complex and had size limitations. Some of those limitations were self-imposed, as the team had decided on a 12-inch-diameter limit to make it easier to attach to a UAV, and easier to insert the device through a hole in the ice floe using the standard boring blade attached to most motorized ice boring equipment.

For phase II, the AECOM team designed a second generation UWID as shown in Figure 17 below. The second generation is a cylindrical shell that has no moving parts while maintaining a 12-inch cross section, yet it can accommodate almost any length to allow more battery storage. The cross section can be reduced to 10 inches in a final commercial version, but the design was left at 12 inches because of the need for working space to accommodate changes in the configuration.

As shown in Figure 17, the new UWID is a long cylindrical shape. Because of the nature of these tests, the design included a 110V-to-24V transformer that allowed the team to switch from an internal, battery-powered operation to an external, 110V configuration with a tether line to an external amplifier and power source. This configuration allowed the team to conduct real-world tests using batteries, but then switch to external power to conduct additional testing using different frequencies, tones and power settings.

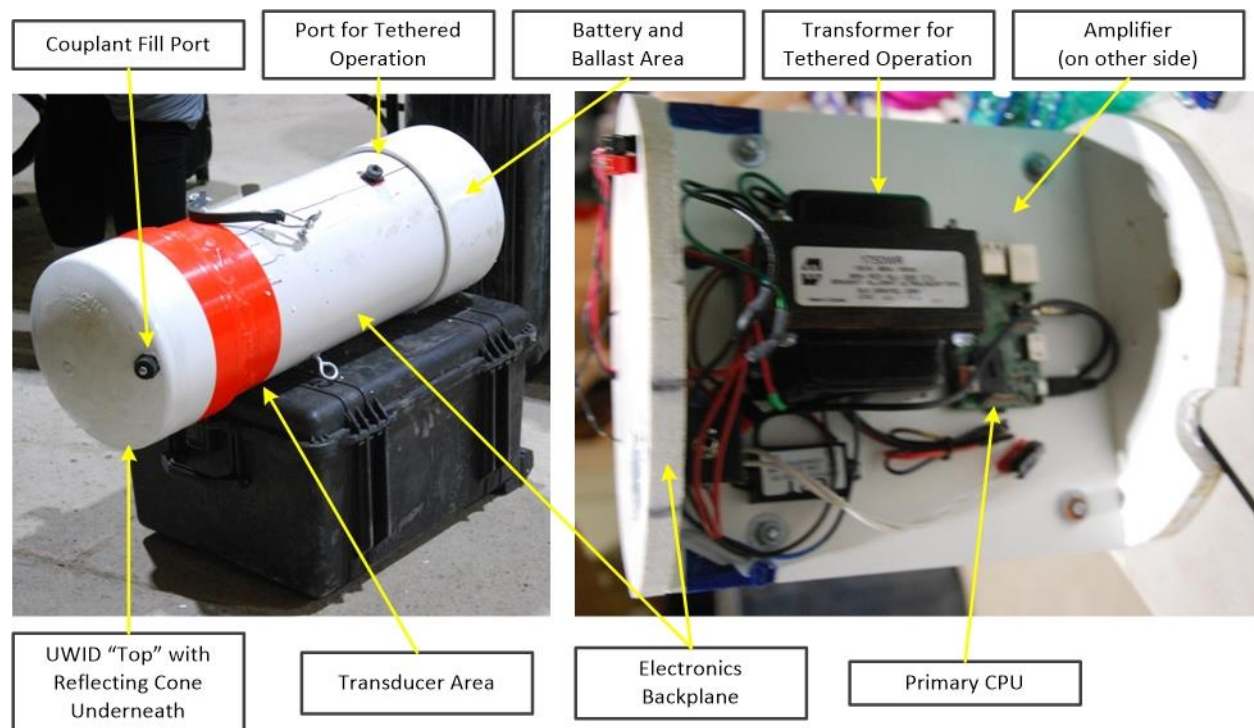


Figure 17: External and internal views of the second generation UWID

The entire UWID is sealed at the top, with a removable bottom cap that allowed the team to switch from battery to external power, change out batteries, make changes to the configuration, and add ballast as needed to balance the UWID to a true vertical profile while in the water and create just enough buoyancy to float up and into the ice floe.

Other components of the UWID tag included:

- a) Body: Thick-walled PVC tubing and end caps.
- b) Couplant: Approximately 12 liters of propylene glycol was used as a couplant in the top of the UWID, filling in the space above the transducer as an acoustic transmissive agent.
- c) Foam reflectors: A two-part urethane foam was used to make the reflecting top cone and the reflecting base underneath the transducer.
- d) Transducer: SX105 bender transducer from Sensor Technologies, 8 inches in diameter, 2.2 inches thick, with a variable frequency range of 400 Hz to 2.5 kHz
- e) Class A/B amplifier: A 400W A/B amplifier for battery-powered operation.
- f) On-board computer with WiFi, allowing the system to be operated without opening the casing.
- g) 110V-to-24V transformer.
- h) Four lead gel batteries at 10 A-hr each.
- i) Ballast as needed.
- j) External amplifier and signal generator: The external amplifier was manufactured by Midstream to provide external power and varying signals for a wide range of testing of UWID signals.

3.3 Second Generation LDGRIDSAT

As show in Figure 18, on the outside the LDGRIDSAT tag had not changed much. The only significant external changes were a slightly smaller cylinder and a 3D-printed cap that was easier to put on and off and provided space for all the antennas located on the top of the LDGRIDSAT tag. The body was still made of a temperature-resistant, thick-walled polypropylene. For the manually deployable version, the ice anchor was still attached to the base with an accelerometer welded to the flange of the ice anchor.



Figure 18: LDGRIDSAT tag deployed on an ice floe in Alaska

Most of the core components between the first and second generation LDGRIDSAT designs remained the same. However, as shown in Figure 19, the inside of the tag was completely redesigned. Instead of hand-cutting the back-plane and supporting structure, the entire inside structure was 3D printed. This provided a more compact structure, built-in shock absorbance for aerial deployments, a concise structure holding the antennas, and an integrated battery compartment. The change to a complete 3D-printed, integrated structure also made it much easier to manufacture and assemble the second generation tags.

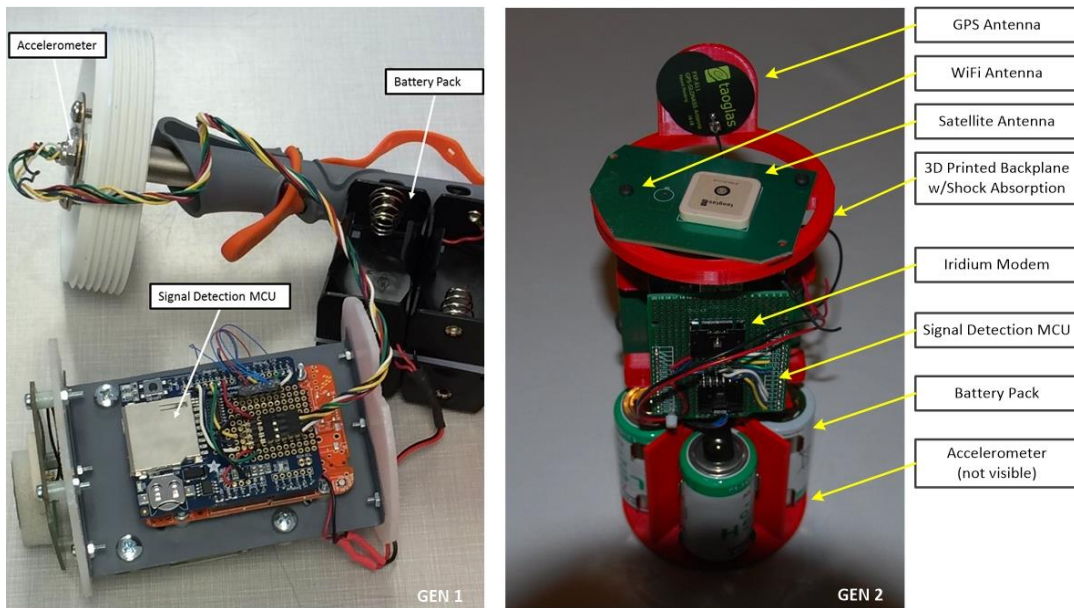


Figure 19: Internal pictures of first and second generation LDGRIDSAT tags

The only change to the internal payload was a change in the accelerometer to a model with a higher sampling rate to better detect the UWID tag. Because of the accelerometer change, and based on the results from the Phase I testing, our team constructed new algorithms for filtering signals received by the accelerometer.

3.4 Remotely Operated Vehicle

As part of Phase II, it was decided that this would be a good opportunity to test the ability for a submersible launch of the UWID. For this test, it was decided to use a lower-cost tethered ROV instead of a more expensive fully remote/untethered UAV. Based on product reviews and interviews with US Navy personnel, our team opted for the Deep Trekker DTX2, a fairly nimble ROV that is easy to transport, and has a very good lighting and camera system and a manipulator claw.

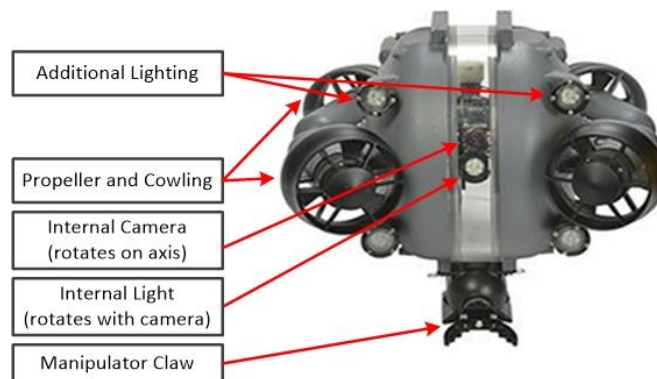


Figure 20: Deep Trekker DTX2 remotely operated vehicle

Our team modified the DTX2 by bolting the UWID harness assembly to the back of the ROV. The UWID harness was essentially a D-ring and nylon string attaching the UWID to the ROV for towing. A neutral-ballast weight was added to the assembly, making the UWID neutrally buoyant during towing, and the weight would drop when the UWID was released from the ROV.

3.5 Cloud Infrastructure and GIS Web Application

Cloud infrastructure provides the backend data acceptance from the satellite gateway, allowing for the processing and interpreting of key tag information such as number of tags in the domain and their locations. After the information is stored in a database, it is available to view through a web application with a map interface showing the locations of tags and their historical readings. Figure 21 diagrams the data flow within the cloud infrastructure. Each element is explained in Section 3.6.



Figure 21: Cloud infrastructure schematic diagram

3.6 Software Tools Employed

The cloud infrastructure consists of the software components listed below, which process the Tag Domain Reports requested from the satellite gateway. They are deployed and run on the Amazon Web Services cloud servers.

- **NginX** – Used as a reverse proxy to manage incoming requests from the gateway. It controls which ports are open and what systems (node application program interface [API], node gateway receiver) can communicate through those ports. NginX works in tandem with the firewall and is also used as the web server for the GIS web application.
- **Node Gateway Receiver** – Listens for packages sent by the satellite, and once received, starts the processing engine. The gateway receiver runs in Node.js.
- **JavaScript Object Notation (JSON) Entity Mapper** – Configuration file used by the node ingestion server to translate the messages into database entities. If the gateway changes protocols or the gateway provider changes, the entity mapper is updated, and the rest of the subsystem should be unaffected.
- **Node Ingestion Server** – Processing engine used to receive incoming messages and translate them into MongoDB database entities. The processing engine runs in Node.js.
- **MongoDB Database** – Used to store the translated entities from the node ingestion server. The database structure defines what the entities are and the data type formats of each attribute in the entities.
- **Apache Solr** – Indexing engine with fast search capabilities.
- **Node API Server** – Runs on the server as the node ingestion server but is used as an API for the mapping application to retrieve and authenticate data from the MongoDB database.
- **Koop** – Data translation engine that can format the database entities into a consumable format for open web-based systems.
- **Turf.js** – Spatial data manipulation engine used to conduct spatial queries and format MongoDB data into GeoJSON.
- **Leaflet** – Web-based GIS mapping user interface that displays interactive features that represent the LDGRIDSATs in the field and the messages and statuses that they send over time.

Cloud-Based Data Servers

The hardware chosen for this project is sufficient for prototyping and proof of concept. Because of Amazon's scalability, what is done on a small scale using its platform can be upgraded to support a larger, production-ready environment. The hardware is suitable to support all software components of this project, including NginX, the node ingestion server, the MongoDB database, and the web mapping application. The Amazon Web Services data centers are staffed 24/7 by trained security guards, contain environmental systems to minimize the impact of disruptions, and span multiple geographic regions to provide resiliency to manmade and natural disasters.

Cloud Infrastructure

The first component of this subsystem is the satellite gateway. The gateway is the conduit for the LDGRIDSATs to relay information from the device to the cloud infrastructure where it is stored. The gateway enables the system to communicate worldwide and outputs information directly into a cloud-hosted database.

The cloud subsystem translates the gateway messages into a normalized format and stores the information in the database. Once the formatted message is received from the gateway, the cloud infrastructure executes the node gateway receiver engine, which parses the message, retrieves all the relevant data needed for the system, and invokes the node processing server.

Amazon cloud servers offer scalability, which means that what is done on a small scale using the platform can be upgraded to support a larger production-ready environment with high availability. The hardware that was chosen is suitable to support all server components of this project, including NginX, node ingestion server and MongoDB database, and is displayed using Leaflet.

Emulator

We also created an emulator to mimic the satellite messages received from the LDGRIDSATs and their associated nodes. This emulator is used to test the message format and integrity of the software components without having to deploy live sensors and use the satellite feed.

GIS Software Application Package

After the NginX reverse proxy accepts the incoming requests from the satellite gateway, the GIS software application package, which consists of the node gateway receiver and processing server, uses the JSON entity mapper to parse the LDGRIDSAT tag, produce Tag Domain Reports, and store the data in the MongoDB database deployed on the Amazon Web Services server. After the data are stored, they are immediately indexed and made available for search using the front end mapping application.

Mapping Application Programming Interface

The user interface is designed to provide all of the desired functionality while maintaining ease of use for novice users. Functionality is as follows:

- LDGRIDSAT tags viewable on a map
- Visible status indicators of LDGRIDSAT tags
- Clickable LDGRIDSAT tags that display additional information about UWID tags
- Reviewable history details for the LDGRIDSAT tags

User guides with detailed step-by-step instructions and screen captures to aid new users are included as Appendices A (LDGRIDSAT Tags) and B (Mapping User Interface) in this report. This application is best viewed in the latest desktop browsers (Firefox 15+, Opera 12.1+, Chrome, Internet Explorer 10+) and mobile platforms (Safari for iOS 3–7+, Android browser 2.2+, 3.1+, 4+, Chrome for Android 4+ and iOS, Firefox for Android, other Web Kit browsers [webOS, Blackberry 7+, etc.], and Internet Explorer 10/11 for Windows devices).

Phase II Updates

There have been several improvements made since Phase I to both the mapping application and the node ingestion server.

- Improved error handling and logging. The gateway and node ingestion server were updated to provide more verbose and detailed logging to troubleshoot errors encountered when receiving, parsing and uploading the data from the messages received from the satellite.
- Improved gateway to manage multi-packet messages. The gateway can now temporarily store and reorder multi-packet messages that are received out of order or that are received staggered between other incoming messages. The satellite messages are capped at a certain size, so long tag reports need to be broken into multiple message packets.
- Email notification for new satellite messages. The node ingestion server is now enabled to send a notification email any time a new message is received by the gateway and successfully inserted into the MongoDB database. In the event that a message was unable to be inserted into MongoDB because of a database error, a notification can also be sent. Both the success and error email notifications are sent to email addresses that are stored in a configuration file and can be updated easily.
- Excel Export functionality. To verify the data received from the satellite, an export function was developed using built-in MongoDB processes. This allows an administrator to export the records stored in MongoDB to a csv file on demand to be used for analysis and reporting.
- Improved “View Detailed Readings” slider accuracy. The “View Detailed Readings” popup in the mapping application shows all of the historical messages and locations for a given sensor. To scroll through the historical data, a slider can be used to traverse a timescale-sorted list of reports. Depending on the distribution of the historical readings, the slider can prove to be fickle. Improvements were made so that the slider scrolls through each historical record in proper sequence and without poor performance due to frequency or distribution of the readings over time.

4. Utqiaġvik Testing and Analysis

The final testing of the Phase II effort of the IFTS was to be in Utqiaġvik on the ice floes in real-world conditions. This testing was conducted, but due to equipment damage and poor ice conditions (see Section 4.2), the testing period was only 8 hours as opposed to the 32 hours originally planned. Because of the curtailment of testing, additional testing was conducted on a frozen lake in Minnesota a year later (see Section 5.0).

The original test was scheduled for March 17, 2018. However, due to the problems with the ROV noted above, the test team had to wait until a replacement ROV could be sent to Alaska. This delayed the testing, which was conducted from March 31 to April 7.

The test objectives were to:

- a) Deploy and test the functionality of the second generation LDGRIDSAT tag, in particular that the LDGRIDSAT tag would log the position of the ice floe and transmit that information through the Iridium network to a cloud-based server, and that the new accelerometers on the LDGRIDSAT tag could effectively receive acoustic signals from the UWID.
- b) Deploy and test the functionality of the second generation UWID, especially its ability to be deployed under the ice by hand and by ROV, and to test that the UWID would orient correctly to transmit acoustic signals up and into the ice floe.

- c) Generate data from the UWID over a variety of settings and distances up to 1 kilometer to test its ability to detect guided acoustic waves through the ice floe.

4.1 Laboratory and Pool

Once Midstream received the ROV, the Midstream and W&M team members tested deploying and driving the ROV in open ponds and at indoor pools at W&M. This included setting up the entire ROV and using the remote control with cold-weather gloves on, test driving the ROV in a clear pool to practice maneuvering and the various options of the ROV controls, test driving the ROV in low-visibility conditions, and testing the UWID harness and deployment of the UWID (see Figure 22).

This testing allowed the team to gauge the ROV's battery strength and longevity before it needed recharging depending on the speed/power used and whether the external lights of the ROV were used. The operational time varied from 1.75 hours with all lights active to 4.0 hours with low-torque settings on the engine and only the camera light active. This testing also allowed the team to test the practicality of towing the UWID and various UWID harness designs. Once a final UWID harness was accepted, the testers continued to practice releasing the UWID and the neutral-buoyancy ballast weight from the ROV, as well as various methods for lowering the ROV and UWID into the water.

However, the Deep Trekker ROV malfunctioned during testing after only 12 hours of use. After working with Deep Trekker, the team learned that one of the circuit boards had malfunctioned. New circuit boards were sent to Midstream, but after several hours of repair attempts, it was determined that it was the main circuit board at fault, and the entire ROV was sent back to Deep Trekker. Deep Trekker was not able to return the ROV in time, so they sent an ROV "loaner" unit directly from their offices to Utqiagvik.

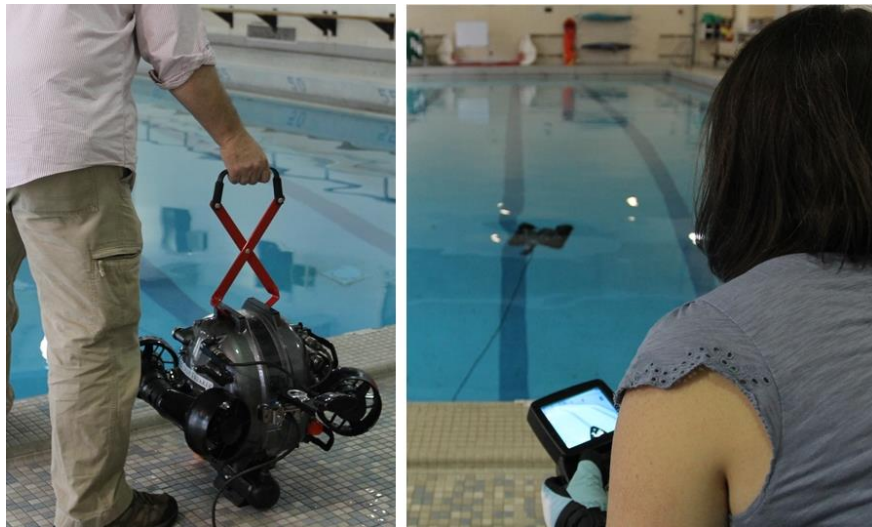


Figure 22: Deploying and test driving the ROV at a W&M pool using cold weather gloves

4.2 Problems Encountered during Testing

During the course of the week, the following problems and issues occurred. These problems cut deeply into the amount of time available for testing.

- Broken ROV: Because of the problem with the ROV noted in Section 4.1, Deep Trekker shipped another ROV directly from their office to Utqiagvik. That ROV arrived with broken cowlings and propellers and internal parts dislodged.

- **Delay in Equipment Arrival:** The equipment was shipped via UPS to arrive in Utqiagvik prior to the test team's arrival. The six boxes of equipment did not arrive until 2 days after the team had arrived.
- **Broken Equipment:** Despite being wrapped in foam, packed in Pelican cases, and the Pelican cases placed in cardboard boxes, it was discovered that almost every Pelican case, and almost everything in them, had been damaged during shipping.
- **Thick Ice/Relocation:** The initial location for testing had an underwater ridge of ice that made the ice too thick to drill through, so a half-day was wasted relocating the test site to ice that we could drill through.
- **Inclement Weather:** While subzero weather is expected in Utqiagvik, the last few days of testing were particularly brutal, with winds in excess of 30 mph and temperatures below -20°F.
- **Encroaching Water:** Despite the cold weather, a channel of water was opening up just 10 miles offshore that continued to open and expand closer and closer to the test site. On the last day of testing, open water was less than 2 miles from the test site.

As discussed, all of these problems combined greatly curtailed the available test period from the planned 32 hours to a total of 8 hours.

4.3 Location, Setup Equipment and Configuration

Testing was conducted approximately 1 mile offshore and 5 miles northeast of Utqiagvik. This test site was within 30 minutes travel of the Ukpeaġvik Iñupiat Corporation (UIC) Science barracks where the test team was housed. The test site was chosen for having a smooth field of at least 1000 m to north before an ice ridge was encountered and having a ridge of about 300 m in one direction to the east. Ice thickness at the test site was about 1.75 m.

The AECOM team used UIC Science, an Alaskan native-owned business, as the outfitter for the testing. UIC Science provided lodging, transportation to and from the airport, a rental vehicle, snowmobiles and sleds for venturing onto the ice, as well as generators, ice boring equipment, ice saws and tents for use on the ice. UIC also provided a guide for the duration of the testing to help with the equipment, set up the test site, and to keep guard for polar bears that may venture close to the test site (see Figure 23).



Figure 23: Setting up the test site on ice floes off the coast of Alaska

Day 1 of testing was supposed to be Sunday, April 1, but the test equipment had not arrived on time. The equipment arrived on April 2 and the day was consumed by receiving and repairing equipment. Additionally, when part of our team went to survey a test site, they found that the initial site chosen was untenable due to a large ridge of ice that made it too thick to drill through. The test site was therefore

moved, and a new hole was created large enough to deploy the UWID and submersibles. The test team measured and marked out distances from the hole (to the right of the tent in Figure 23) where the UWID acoustic reception would be tested, and that ended the day on the ice.

On Tuesday, April 3, the test team deployed both the tethered “kayak” system and the UWID without the ROV, as the ROV was still being repaired. The team used both UWID variants (the tethered accelerometer for raw data collection for signal processing [Figure 24] and the standalone LDGRIDSAT tag) to support data collection over multiple hours each day. During the test setup, it was found that the amplifier used in tethered testing, which initially appeared to be in working condition, was also broken during shipment, and that required the rest of the day to repair. It was also discovered that a voltage transformer in the UWID was not operating correctly, so that also had to be repaired.



Figure 24: Deployment of the tethered UWID under the ice floe

During testing throughout the week, a tethered accelerometer was used concurrently with a LDGRIDSAT tag, as shown in Figure 25. The tethered accelerometer is at the base of the gray tubing next to the LDGRIDSAT tag, so both distances and site were identical for comparing data.



Figure 25: A tethered accelerometer and LDGRIDSAT tag

The first actual day of testing was Wednesday, April 4. Because of delays, the hole into the ice floe had to be re-opened causing additional delays. Both the tethered UWID and the second generation UWID were finally able to be deployed, and initial calibration and short-range testing commenced.

On Thursday, April 5, we were able to use the ROV. The ROV was operational but auto-depth and auto-direction capabilities had not been restored. After we deployed the ROV, we found that it could not maintain a straight heading, probably due to a miscalibration of the damaged thruster, which in turn compromised the auto-course capabilities. Despite this, we were still able to deploy the ROV-UWID, and we did prove that the towed configuration would work with a submersible in deploying the UWID under the ice floe (Figure 26).



Figure 26: Deployment of the UWID using an ROV

On April 5, we deployed one of the LDGRIDSAT tags on the ice floe for testing after we left. However, we lost communication with the tag via satellite shortly after we left. UIC Scientific, our outfitter, returned to the test site on April 11 and confirmed that water had encroached into the test site and that the LDGRIDSAT tag could not be found.

The team had considered staying extra days on the ice for testing, but open water had consistently encroached during the week, and was only 2 miles from the test site on April 6, so the test site was abandoned and all equipment returned to the staging area at UIC Science.

4.4 Data Collection

Data was collected via several methods comprising written notes of all UWID settings, serial transmission from the tethered accelerometer to a computer, WiFi from the LDGRIDSAT tags, and satellite communication with the LDGRIDSAT tags. A test grid had already been marked off for 10 m, 20 m, 30 m, 40 m, 50 m, 100 m, 250 m, 500 m and 1000 m. As testing progressed, the tethered accelerometer and LDGRIDSAT tag were moved to the next distance, and then the team turned on the tethered or second generation UWID to transmit into the ice floe for detection.

Data capture Included:

- Latitude and longitude, ice thickness, general condition of the ice at the testing site location, and meteorological conditions.
- UWID (tethered and untethered) location, local time, and signal generated (frequency, power and pulse length).

- LDGRIDSAT configuration by ID and position relative to UWIDs. Satellite message reports from the GIS user interface that includes latitude and longitude, UWID detections and time stamp.
- Accelerometer locations relative to UWIDs. Raw data capture of meters per second squared versus seconds, recording the local time window of the data collected.

Data capture parameters are summarized in Table 1.

Table 1: UWID Settings, Test Data Collection, and Detection Determination

Date	Local Time	UWID Type	Number of Tests	Power Setting	Distance from UWID (m)	Detection
4/4/2018	11:30 a.m.	Tethered	3	25	5	No
	11:45 a.m.	Tethered	3	50	5	No
	12:00 a.m.	Tethered	3	100	5	No
	12:15 a.m.	Tethered	3	25	10	No
	12:30 a.m.	Tethered	3	50	10	No
	12:45 a.m.	Tethered	3	100	10	No*
4/5/2018	12:00 p.m.	Tethered	2	25	30	Yes
	12:15 p.m.	Tethered	2	50	30	Yes
	12:30 p.m.	Tethered	4	100	30	Yes
	2:00 p.m.	Tethered	2	25	40	No
	2:30 p.m.	Tethered	2	50	40	Yes
	2:45 p.m.	Tethered	4	100	40	Yes
	3:15 p.m.	Tethered	3	25	50	No
	3:30 p.m.	Tethered	3	50	50	No
	3:45 p.m.	Tethered	3	100	50	Yes
4/6/2018	12:15 p.m.	Untethered	4	100	10	Yes
	12:45 p.m.	Untethered	2	100	20	No**
	1:15 p.m.	Tethered	10	100	5	Yes
	1:45 p.m.	Tethered	15	75	10	Yes
	2:15 p.m.	Tethered	15	100	20	Yes
	2:45 p.m.	Tethered	15	100	25	Yes

*Amplifier or UWID inoperable

**Untethered UWID started taking on water

4.5 Analysis

To localize the UWID from the recorded waveforms, it was necessary to identify the UWID signal arrivals even when they were buried deeply in noise. For the Barrow data, we employed both a time-domain cross-correlation method that uses the repeating tone burst structure of the transmissions and a 2D image convolution method based on a wavelet transformation [7]. Four waveforms recorded during the 2018 Barrow tests were used for comparison. Figure 27 depicts the raw data recorded from the accelerometer of the second generation UWID. This pattern is typical of recordings made on the ice and initial acoustic signals, but also shows reflections of the signal by the bottom of the ocean and possible reflections from ice ridges. This recording lasted about 350 seconds, or 5 minutes and 50 seconds, to ensure that the recording contained at least 1 of the 30-second periods for which the signal was being generated.

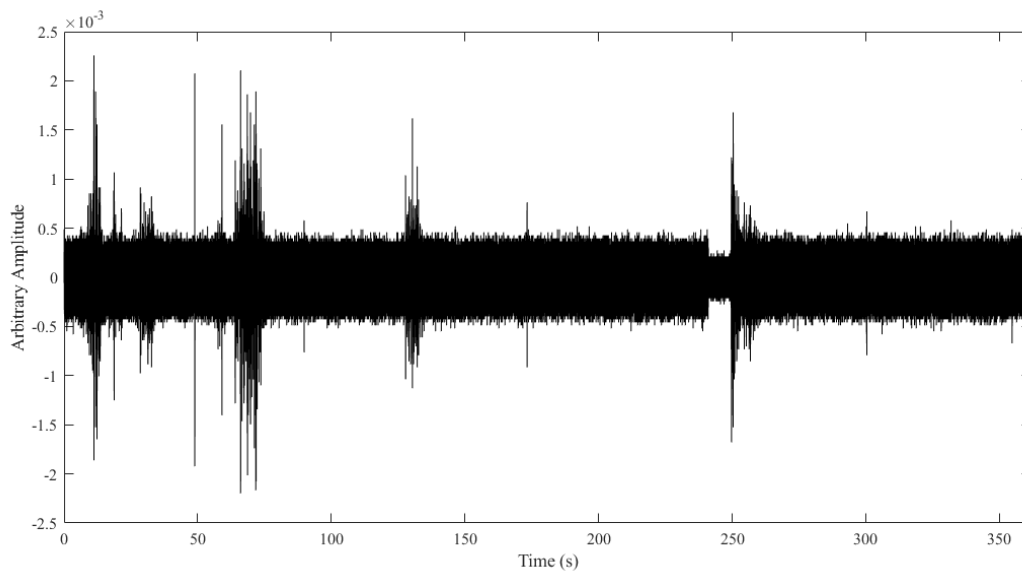


Figure 27: Unfiltered topside recording of the signal from the untethered UWID

Figure 28 shows the results of isolating the signal with bandpass filtering to isolate the 1 kHz signal used by the untethered, second generation UWID. The UWID was set to transmit a sequence of 1 kHz tones, which allowed us to apply a bandpass filter to the topside recordings in the frequency domain. We took an FFT, then multiplied the data by an array containing only the frequencies we were interested in, from 950 Hz to 1050 Hz. We then took an inverse FFT to obtain the filtered signal. The top left plot in Figure 28 is the raw recording where the x-axis is time in seconds and the y-axis is the amplitude. The top right plot is the frequency content of the raw recording, where the x-axis is frequency in hertz and the y-axis is amplitude. Here there is a clear peak at 1 kHz, showing that we did detect the signal from the UWID. The bottom left plot shows the filtered frequency spectrum. The bottom right plot shows the filtered signal, where the signal of interest is not immediately apparent.

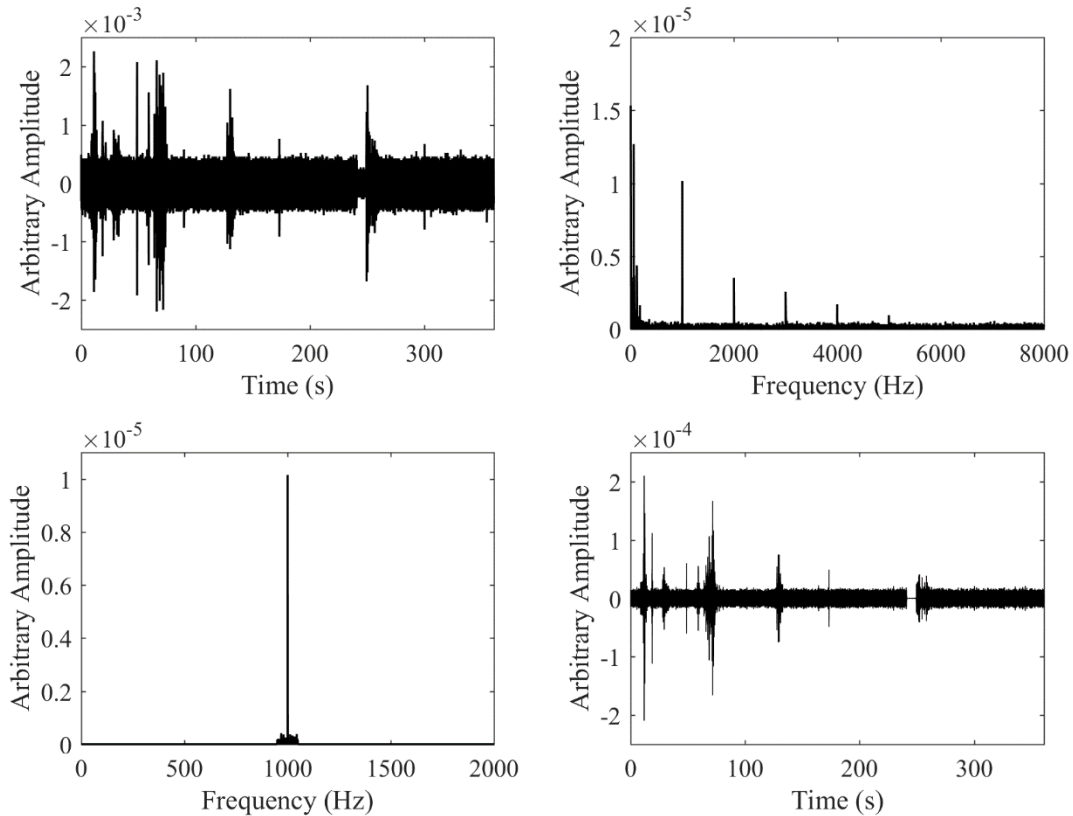


Figure 28: Bandpass filter isolates 1 kHz signal

We then performed signal processing on the data to help identify the arrival time of the Lamb waves so that the UWID source location could be determined. We first implemented a time-domain cross-correlation method to identify the signal. For this method, we created a synthetic signal that replicated the signal recorded directly from the UWID immersed in a small water tank in the laboratory. We then performed the cross correlation between the topside recordings and these synthetic signals of various lengths. Figure 29 shows the cross correlation between the first topside recording using the untethered UWID filtered around 1 kHz and the synthetic signal containing 10 tone bursts. The red line indicates the maximum of the cross correlation where the signals are the most similar. We were also able to overlay the synthetic signals onto the filtered recording and zoom-in to look for the repeating tone-burst structure that the UWID was transmitting. The bottom plot shows the filtered topside recording in black overlaid with the synthetic signal containing 10 tone bursts in red starting at the time step identified by the cross correlation.

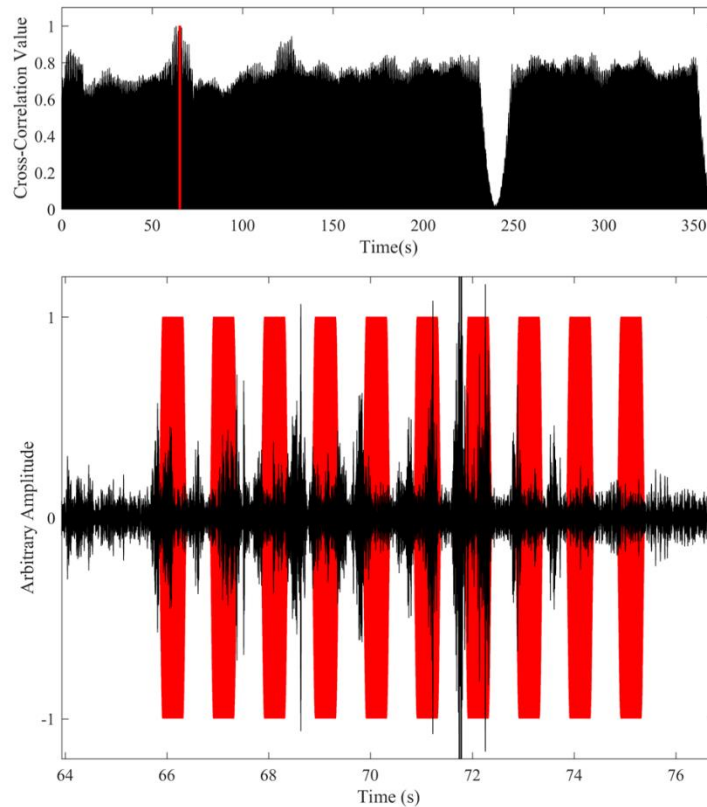


Figure 29: Cross correlation results

The obvious signal processing approach for the application was to use a narrow bandpass filter followed by peak detection. Advanced signal processing methods were necessary, however, because the signals we recorded were quite complex. Furthermore, identifying the UWID signal at large propagation distances means those signals are always going to be buried in the noise, and the “fingerprint” of the signal will usually be quite subtle.

Consequently, we chose to use the dynamic wavelet fingerprint technique (DWFT) to narrow down the arrival time of the signal. DWFT uses wavelet transform coefficients to render an image similar to the spectrogram, except that the vertical axis is wavelet scale instead of frequency. The horizontal axis is still time delay because the wavelet shift corresponds to that directly. By converting the one-dimensional signal into a two-dimensional image, subtle features can be extracted that other methods may miss.

By using DWFT, we were able to use computer vision techniques to identify the arrival time of the Lamb waves. We used 2D image convolution to find local patterns in images by using a kernel image that represented a pattern of interest and sliding it across the image. At each step, the kernel image and the corresponding section of the larger image were multiplied element-wise and summed, resulting in a number representing how similar the two are; the larger the number, the more similar they are, as illustrated in Figure 30. Using the results from the cross-correlation analysis as a baseline, we performed DWFT analysis to try to better localize the UWID signal in the recorded waveforms. To do this, we ran a two-dimensional convolution using DWFTs of the synthesized output signal and the denoised recorded signals. We used a stride of 0.1 second such that we shifted the kernel image by 4410 samples. Figure 31 (top) shows recording 1 denoised. The middle plot in Figure 31 shows the 2D convolution with the denoised waveform of recording 1, and the synthetic signal.

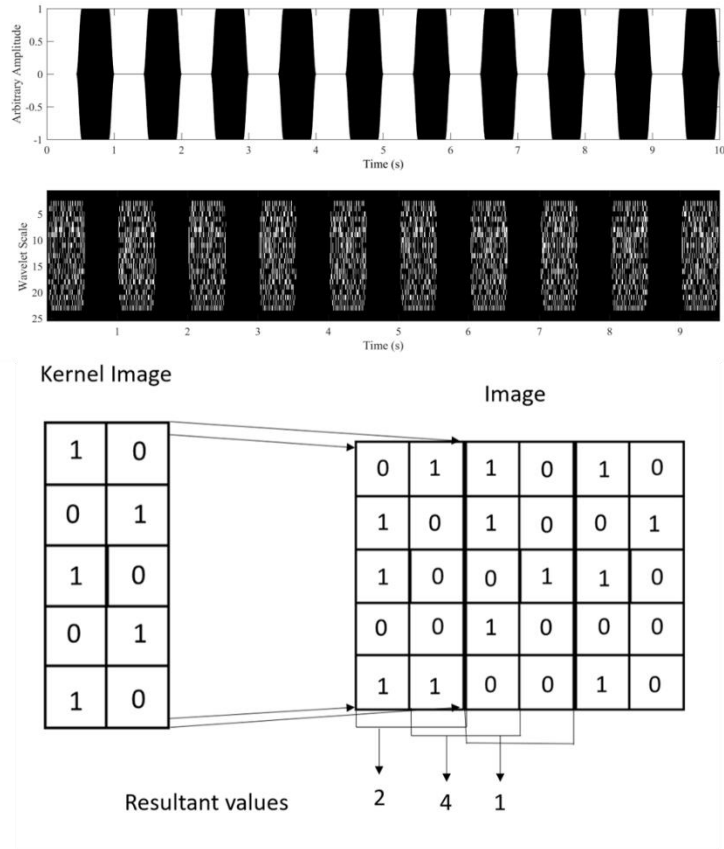


Figure 30: Dynamic wavelet fingerprint and kernel used for 2D analysis

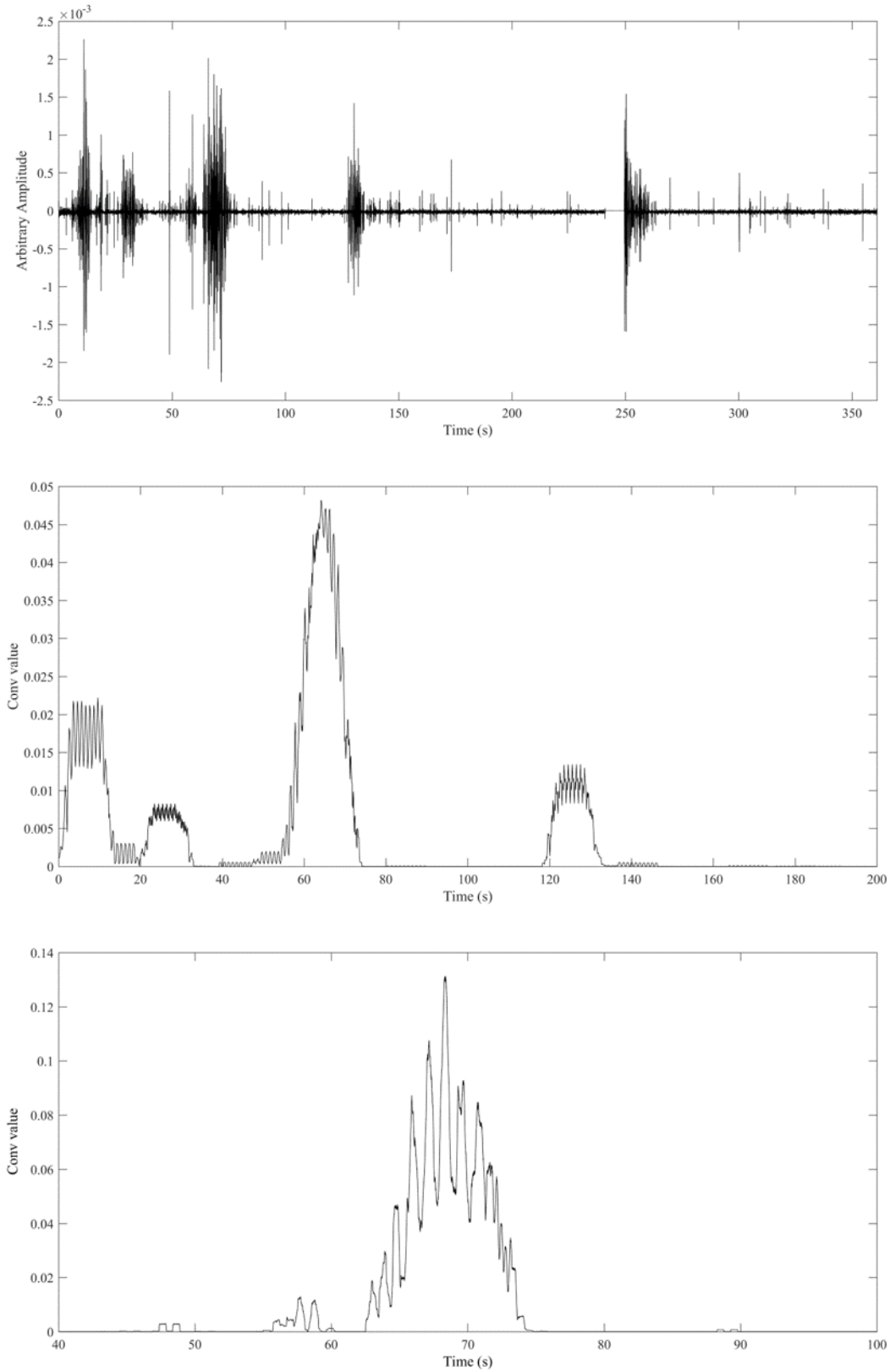


Figure 31: Denoised signal, convolution using 10 seconds of UWID pulse as the kernel, and convolution using 2-second pulses as the kernel

The time-domain cross-correlation technique uses the known structure of the transmitted signal to identify signal arrivals. Synthetic signals of varying lengths that mimic the repeating 1 kHz tone-burst signal are used in that cross-correlation and give a way to isolate the regions of the signal that warrant further analysis. The team conducted a follow-on analysis with a 2D convolution in a wavelet transform domain, which allows for sequentially zooming in to identify the signal arrivals with high enough accuracy for triangulation by the LDGRIDSAT system. Convolution values were indeed quite low, but the wavelet fingerprint method was still able to find locations that were likely to contain the signal of interest buried deeply in noise and/or signal distortion inherent in real-world tests. Identifying signal features of interest even when they are buried too deeply in noise for other methods is a strength of this technique. For more detail on the analysis process, please refer to Skinner et al. [7].

Table 2 shows the LDGRIDSAT detecting the three UWID tag report pulses prior to sending a gateway report message to the GIS web application as verified by the accelerometer (Table 1).

Table 2: LDGRIDSAT Report

Date	Distance (meters)	GPS Report Time	Number of UWID Reports
4/5/2018	20	2:46	3

This LDGRIDSAT gateway report is shown in Figure 32 below.

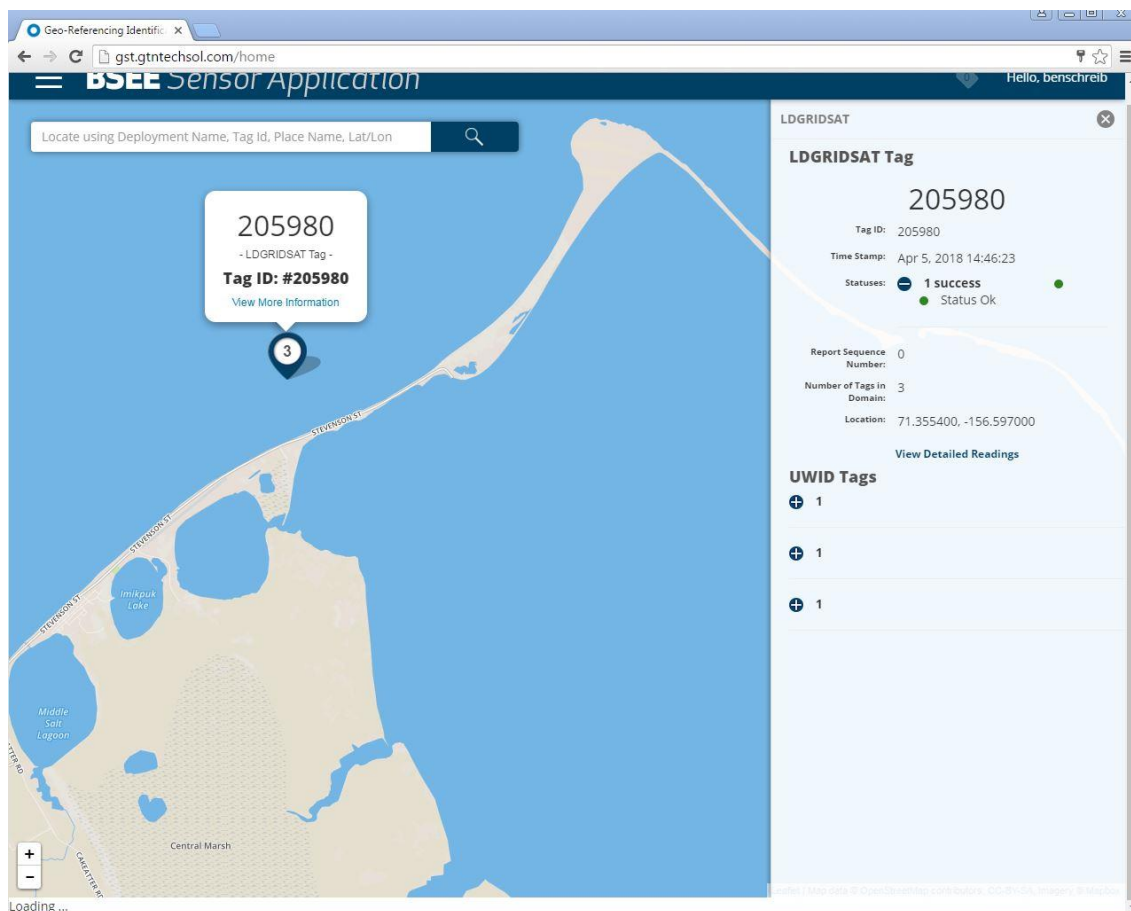


Figure 32: LDGRIDSAT tag gateway report from the test site off the coast of northern Alaska

5. Cass Lake, MN, Testing and Analysis

Due to problems with test equipment and conditions in Utqiagvik (Barrow), Alaska, the AECOM team was not able to collect as much data as they would have liked for the IFTS, especially long-range testing of the UWID tags. The AECOM team led by Midstream Technology conducted additional testing of IFTS on lake ice at Cass Lake, Minnesota, in mid-February 2019.

5.1 Location, Setup Equipment and Configuration

The test team consisted of Sam McClintock, Ted Hale, and Elizabeth Skinner. They drove the equipment to Cass Lake starting on February 13, and tested Saturday, February 16 through Tuesday, February 19. Wednesday and Thursday had been reserved for additional testing but were not needed. The lodging and support on the ice was provided by the Wishbone Resort, who provided cabins and an ice fishing shelter that was converted for the testing.

The testing was conducted on Cass Lake, which had sufficient ice (2 to 3 feet thick) to support vehicles and shelters. The weather was relatively clear with light winds during the testing, with temperatures ranging from -17°F to +15°F. The central test location where the UWIDs were deployed was 47°26'40"N 94°35'04"W, about 1 kilometer south by southwest of the resort's shoreline (Figure 33).

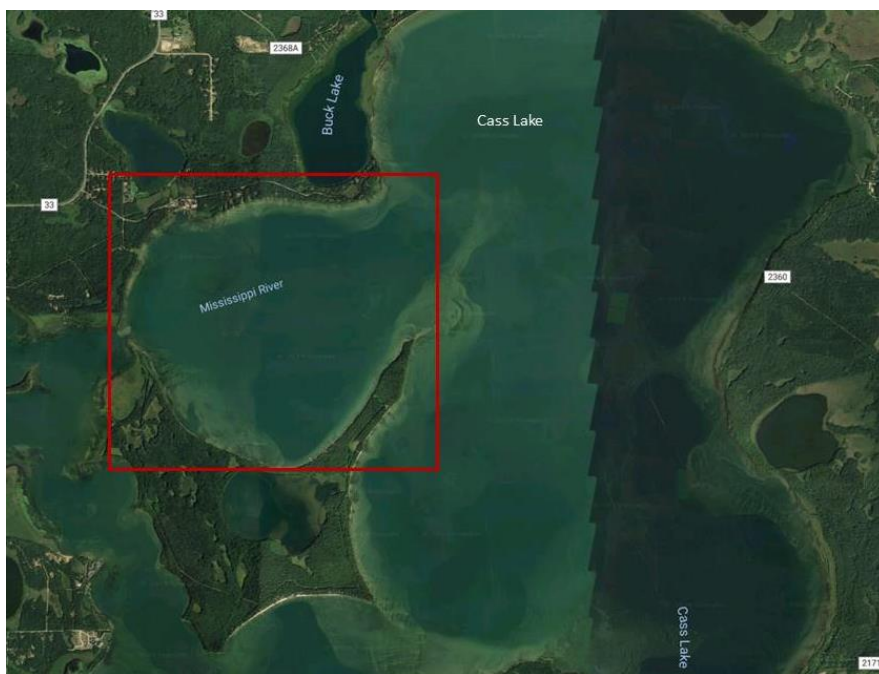


Figure 33: Area of Cass Lake where IFTS testing was conducted

The team originally started marking a test grid to place acoustic receivers to the southeast of the test location that had about 3 kilometers of free ice. However, because of heavy snow on the ice, which acts as an insulator, the bottom layer of snow became slush and very hard to walk or drive through. Short-range testing through 200 m was conducted to the southeast, but longer-range tests through 1.2 kilometers were conducted due east (with 6 kilometers of free ice in that direction), where it was easier to set up test locations. Figure 34 shows the test site location and direction of the test grids.



Figure 34: Test site and direction of LDGRIDSAT and accelerometer placement

5.2 Data Collection

Two different types of UWID tags were deployed under the ice:

- The first-generation "kayak" design that transmits acoustic waves omni-directionally into the ice.
- The second-generation UWID tag first used in the Arctic testing in 2018. It uses a foam cone to project the acoustic energy into the ice at a critical angle to generate Lamb waves.

The acoustic signals transmitted through the ice were generated using Midstream's custom-built amplifiers. These signals were varied by the length of the tone bursts, power to the transducer, and frequency (1 to 3 kHz).

The team deployed four accelerometers on the top side of the ice to detect the UWID acoustic signals, with most of the data collected using Digiducer's Model 333D01 Digital Accelerometers. Data were collected at 1, 10, 20, 30, 50, 100, 150, 200, 500, 1000 and 1200 meters from the UWID tags. During the course of the 4 days on the ice, our team conducted over 500 separate tests.

5.3 Analysis

Using the UWID, we propagated two types of acoustic signals: a tone burst and a longer pure tone. Most of the tone bursts we generated consisted of approximately 15 cycles of a sinusoidal wave with a pulse repetition rate of 0.11 second. We also took some data using longer tone burst with up to 50 cycles per burst and a pulse repetition rate of 0.15 second. At distances over 500 meters, we also took data using pure sine wave tones that were played for 1 minute. By using longer tone bursts and pure sine wave tones we increase the chances of picking up the signal. This is because the longer the tone, the more acoustic energy is contained in the signal. Having more energy in the signal increases the distance that the signal can propagate and therefore increases the chances of detection at longer distances.

Our testing was able to detect both UWID tags. Table 3 shows the UWID test settings. Table 4 shows the types of test performed. The detection range varied by power, frequency and tone burst length. Figure 35 shows the frequency content of collected data for one of the tests at 1.0 kilometer. The x-axis is the frequency in hertz and the y-axis is arbitrary amplitude of the frequency content. The plot shows the frequency content when the 1-minute, 2.6 kHz pulse was transmitted from the UWID. Here peaks at 1, 2, 3, 4 and 5 kHz show harmonic noise in the system that is present in all the data. The plot shows a clear peak above the noise floor at the frequency at 2.6 kHz showing detection of the acoustic signal at 1 kilometer. This peak is highlighted by the blue rectangle, and the small plot in the corner is zoomed into the region of interest.

Table 3: UWID Test Settings and Detection Confidence

Date	UWID Type	Distance	Testing Pattern
2/16/19	Kayak	1 meter	A, B
2/16/19	Kayak	10 meters	C
2/16/19	Kayak	20 meters	C
2/16/19	Kayak	30 meters	D
2/17/19	Pill	1 meter	E
2/17/19	Pill	10 meters	E
2/17/19	Pill	20 meters	E
2/17/19	Pill	30 meters	E
2/17/19	Kayak	40 meters	F
2/17/19	Kayak	50 meters	F
2/17/19	Kayak	500 meters	F
2/17/19	Kayak	1000 meters	F
2/17/19	Kayak	1200 meters	G
2/18/19	Kayak	100 meters	H, I
2/18/19	Kayak	150 meters	H, I
2/18/19	Kayak	200 meters	H, I
2/18/19	Kayak	500 meters	H, I
2/18/19	Kayak	1000 meters	H, I, J
2/18/19	Kayak	1200 meters	H, I, J
2/19/19	Pill	10 meters	K
2/19/19	Pill	1200 meters	L, M
2/19/19	Kayak	500 meters	N
2/19/19	Kayak	1000 meters	O
2/19/19	Kayak	1200 meters	P

Table 4: Types of UWID Tests Performed

Testing Pattern	Description	Power Settings
A	1 kHz, increasing the number of cycles in tone bursts	50%
B	15 cycles per tone burst <ul style="list-style-type: none"> • 1.21, 1.42, 1.6, 1.75, 2.02, 2.23, 2.41, 2.7 and 3.11 kHz • sweeping frequency slowly from 0.95 to 4.1 kHz 	50%
C	15 cycles per tone burst <ul style="list-style-type: none"> • 1.75, 2.02, 2.23, 2.46 and 2.7 kHz • sweeping frequency slowly from 0.95 to 4.1 kHz 	50%
D	15 cycles per tone burst <ul style="list-style-type: none"> • 1.75, 2.02, 2.23, 2.46 and 2.7 kHz • sweeping frequency slowly from 0.95 to 4.1 kHz Frequency 2.37 kHz <ul style="list-style-type: none"> • sweeping cycles in tone burst slowly from 5 to 50 kHz 	50%
E	15 cycles per tone burst <ul style="list-style-type: none"> • 1.75, 1.87, 2.02, 2.23, 2.46, 2.7, 3.11 and 3.58 kHz • sweeping frequency slowly from 0.95 to 4.1 kHz 50 cycles per tone burst <ul style="list-style-type: none"> • sweeping frequency slowly from 0.95 to 4.1 kHz 	50%
F	15 cycles per tone burst <ul style="list-style-type: none"> • 2.02, 2.11, 2.15, 2.23, 2.3, 2.46, 2.55, 2.7 and 2.9 kHz • sweeping frequency slowly from 0.95 to 4.1 kHz 50 cycles per tone burst <ul style="list-style-type: none"> • sweeping frequency slowly from 0.95 to 4.1 kHz 	50%
G	Sweeping frequency slowly from 0.95 to 4.1 kHz <ul style="list-style-type: none"> • 15 cycles per tone burst • 50 cycles per tone burst 	
H	2.23 kHz <ul style="list-style-type: none"> • 15 cycles per tone burst • 35 cycles per tone burst • 50 cycles per tone burst 	50, 70, 90%
I	10 cycles per tone burst <ul style="list-style-type: none"> • sweeping frequency slowly from 0.95 to 4.1 kHz 	90%
J	1-minute tones from 1 to 3 kHz by 0.2 kHz	90%
K	15 cycles per tone burst <ul style="list-style-type: none"> • 2.55, 2.7 and 2.9 kHz 	50%

Testing Pattern	Description	Power Settings
L	2.55 kHz <ul style="list-style-type: none"> • 15 cycles per tone burst • 35 cycles per tone burst • 50 cycles per tone burst 2.77 kHz <ul style="list-style-type: none"> • 15 cycles per tone burst • 35 cycles per tone burst • 50 cycles per tone burst 	50, 70, 90%
M	2.9 kHz <ul style="list-style-type: none"> • 15 cycles per tone burst • 35 cycles per tone burst 	50%
N	<ul style="list-style-type: none"> • 1-minute tones from 1 to 2 kHz by 0.2 kHz • 1-minute tones from 2 to 2.8 kHz by 0.1 kHz • 1-minute tone at 3 kHz 	70, 90%
O	<ul style="list-style-type: none"> • 1-minute tones from 2.2–2.7 kHz by 0.1 kHz 	50, 70, 90%
P	Tones 2.2 to 2.8 kHz by 0.1 kHz <ul style="list-style-type: none"> • 1 minute • 30 seconds • 15 seconds 	50, 70, 90%

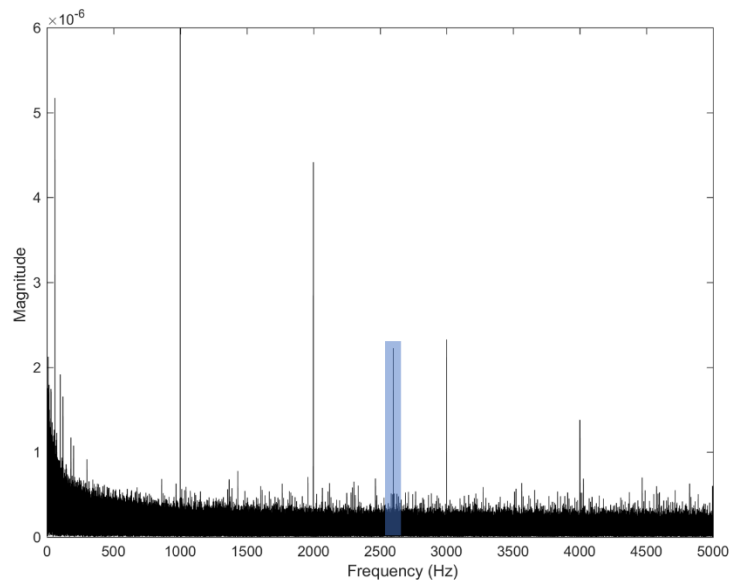


Figure 35: Detection of UWID signal at 1 kilometer

6. Commercialization Plans

LDGRIDSAT production can be started and quickly increased for commercial sales. The question is how many of these tags would be ordered in 1 year. Yearly sales of >500 units would justify further cost reductions such as integrated circuit design and transducer housing improvements. If the sales were less, then it would remain a more “manual” process with 3D printing of the backplane and body and assembly of the integrated circuit.

Oil production-related applications in the Arctic are the predominant use cases, and the most likely customers are those companies supporting incident response to North Slope oil and gas production, pipelines, and Equinor (formerly Statoil) operations in the Arctic. Over the next decade we will see increased commercial cargo traffic, including oil tankers, in Arctic routes, which may also develop an additional customer base for LDGRIDSAT tags.

7. Conclusion

The IFTS concept and testing has demonstrated that ice floes can be tracked with a relatively low-cost tracking tag. The LDGRIDSAT tag design ensures survivability of aerial drops and can be deployed in a manual mode as well. The tags are of a size that 10 or more can be easily stored for use for several years until they are needed. The use of the Iridium polar-orbiting network means that the tags can communicate from anywhere in the world, so the tags would also be useful to other countries and companies operating in extreme latitudes. The LDGRIDSAT can be produced commercially without extensive modification and can be in the hands of response teams within months of placing an order.

The concept that acoustic guided waves can be detected at distances up to 1 kilometer was proven, so the UWID works, and it can be placed into commercial production. However, our team believes the demand for these tags will be low and that only 10 to 20 of the tags may ever be produced. While the UWID can be produced commercially, because of power requirements for extended detection ranges, it is probably better to integrate the transducer with the UAV using the UAV’s on-board computer and battery, and have the UAV approach the ice to generate a signal. Then the UAV can return and recharge prior to the next mission.

8. References

- [1]. A. Peiffer, B. Köhler, and S. Petzold, "The acoustic finite integration technique for waves of cylindrical symmetry (cafit)," *Journal for the Acoustical Society of America*, vol. 102, pp. 697-706, Aug. 1997.
- [2]. B. Schreib, Alex Bostic, Jarrett Mitchell, Alin Nomura, Manuel Sanchez, Jason Lin, Sam McClintock, Ted Hale, Navid Yazdi, David Rein, George Meng, Casey Wallace, Elizabeth Skinner, and Mark Hinders, "Tagging of oil under ice for future recovery final report," Final Technical Report E14PC00028, BSEE, Aug. 2016. <https://www.bsee.gov/sites/bsee.gov/files/research-reports//1051aa.pdf>.
- [3]. N. Patrikeeva and P. Sava, "Comparison of angle decomposition methods for wave-equation migration," *Society of Exploration Geophysicists*, 2013.
- [4]. K. Yoon and K. Marfurt, "Reverse-time migration using the poynting vector," *Exploration Geophysics*, vol. 37, pp. 102-107, 2006.
- [5]. A. Richardson and A. E. Malcolm, "Separating a wavefield by propagation direction," *Geophysics*, vol. 81, no. 3, pp. T117-T129, 2016.
- [6]. T. A. Dickens and G. A. Winbow, "RTM angle gathers using pointing vectors," *SEG Technical Program Expanded Abstracts*, pp. 3109-3113, 2011.
- [7]. E. D. Skinner S. L. Kirn, and M. K. Hinders, "Development of underwater beacon for Arctic through-ice communication via satellite," *Cold Regions Science and Technology*, vol. 160, pp. 58-79, 2019.

Appendix A – LDGRIDSAT Tag Operations and User Guide

LDGRIDSAT

The following sections summarize the components, procedures and settings for operation of the LDGRIDSAT tag.

Setup

Before using the systems, the user activates the satellite data service plan on the LDGRIDSAT units through an authorized service provider. The modem number (IMEI) will need to be provided. The satellite data are routed to the pre-defined cloud infrastructure server IP address and port number.

To communicate with the LDGRIDSAT in Maintenance Mode via USB, the appropriate USB driver will have to be installed on the PC. This can be provided or downloaded directly from the vendor website.

Startup

To install or replace the battery, the bottom cover of the LDGRIDSAT tag must be unscrewed to expose the battery compartment as shown in Figure A1. Once the batteries are installed and the cover is replaced, the tag will start functioning autonomously; the tags do not have an external power button. Tag IDs are assigned as factory default and are imported into the cloud infrastructure database as part of the standard tag messages.

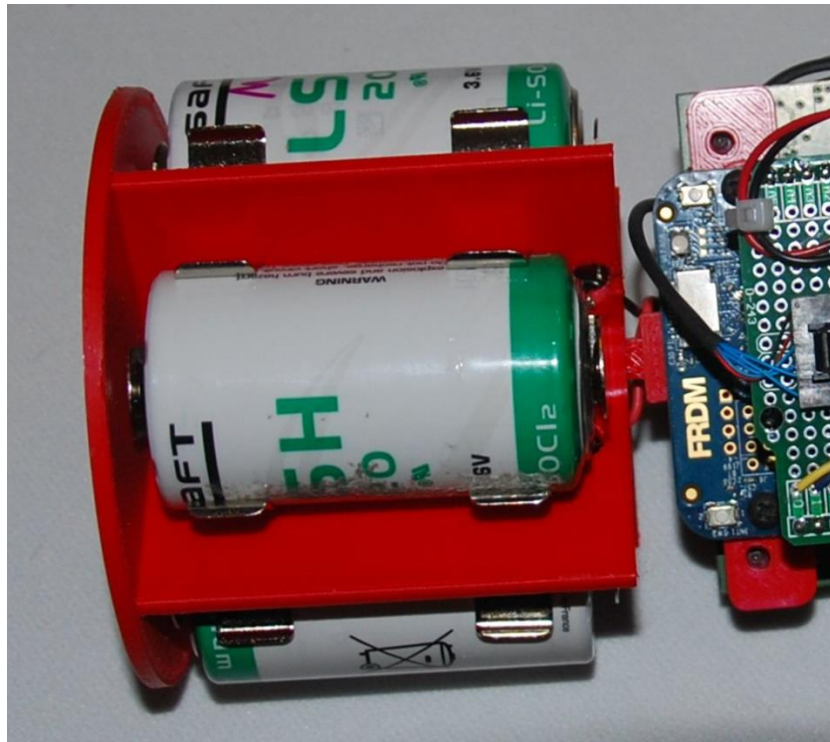


Figure A1: LDGRIDSAT tag startup and configuration component parts

Configuration

The LDGRIDSAT tag does not have any external buttons and it operates autonomously. The UWID tag does not have any external buttons and operates in an active mode. In this mode, the UWID tags produce an acoustic beacon that the LDGRIDSAT tags detect when in active mode.

The LDGRIDSAT tag operates in two different modes:

- Active Mode.** This is the mode in which the tags operate during deployment. In this mode, the LDGRIDSAT tag acts as a network-coordinator host to receive acoustic beacons and process data to ascertain the presence of UWID tags. The LDGRIDSAT tag also establishes the satellite communication link and runs the server update cycle with GPS fix.
- Maintenance Mode.** This mode can be initiated by issuing an addressed maintenance command message to a target LDGRIDSAT tag through the USB interface (type-A male USB-to-mini type-B male USB cable required). In this mode, the configuration parameters on the tags can be retrieved and set using command messages.

Maintenance Mode is used to configure tag parameters. To enter Maintenance Mode:

- Plug in the USB cable to the unit and PC.
- Insert batteries into the battery holder. The USB device should show up as a serial port within Windows device manager (if not, ensure that the appropriate USB drivers have previously been installed on the PC).
- Start TeraTerm (or any terminal emulator). Select the following serial port parameters:
 - Port: Determine the port that the device has been assigned (through device manager) and select it from the drop-down box
 - Baud Rate: 115,200 bps
- Press the “?” key to get a menu to print.
- Enter the desired commands or configuration parameters. The settings will be retained until the LDGRIDSAT batteries are depleted or removed.

The configuration parameters and the screen shot of the maintenance software tool are presented in Table A1 and Figure A2.

Table A1: LDGRIDSAT Configuration Parameters

Command	Description	Parameter
P (shift-P)	Sets the LDGRIDSAT automatic reporting period.	Valid range: 0 – 10,080 minutes. 0 disables the automatic reporting.
r	Manually transmit an LDGRIDSAT report (when P=0). Will attempt to transmit all collected UWID tag information via satellite link.	N/A
R (shift-R)	Manually transmit an LDGRIDSAT report with test UWID data. This is useful for testing the LDGRIDSAT satellite link quality.	Number of UWID report entries to generate.
D (shift-D)	Enable diagnostic output. Will display UWID report entries as acoustic beacons are received.	N/A
d	Disable diagnostic output.	N/A

Command	Description	Parameter
v	Display firmware version and LDGRIDSAT serial number.	N/A
g	GPS Monitor – manually get and display GPS fix.	N/A
I (shift-I)	IMEI Read – display the IMEI of the satellite modem.	N/A

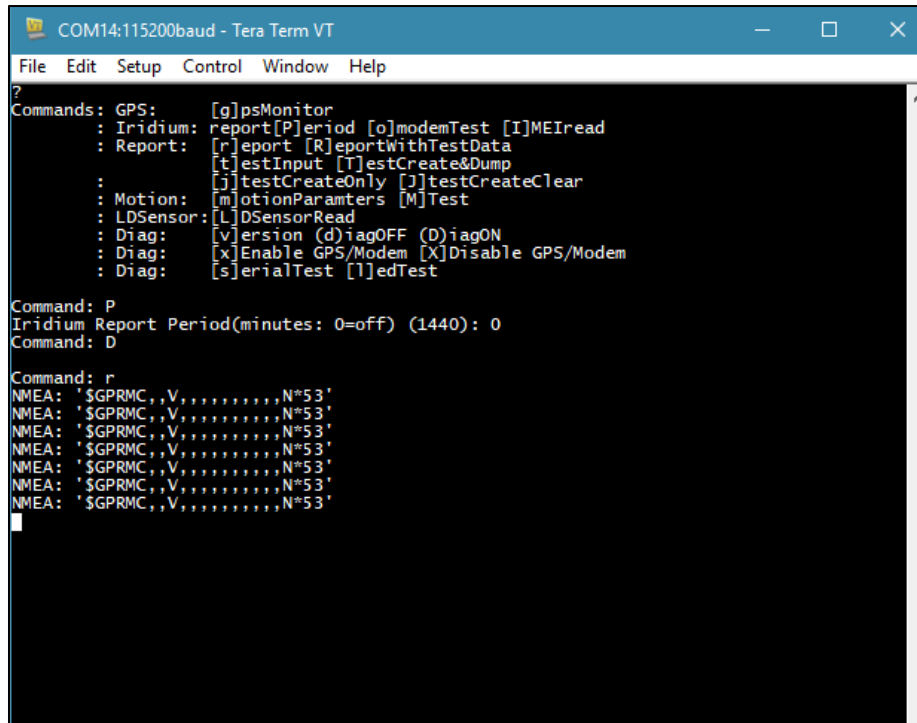


Figure A2: TeraTerm command line interface to configure and test LDGRIDSAT hardware

To disconnect and power down from Maintenance Mode:

1. Go to TeraTerm File tab and click disconnect or close TeraTerm.
2. Unplug the USB cable. The LDGRIDSAT will continue to run under the set configuration if batteries remain inserted and have not depleted.
3. To power the unit down, remove the batteries from the system. This will wipe out any data or configuration and reset to the default when powered back on.

Appendix B – Mapping User Interface User Guide

1. Application Overview

- a. The BSEE Sensor Application enables remote stakeholders to view data from Lamb-wave Detection Geo-Referencing Identification Satellites (LDGRIDSATs) via a satellite network and web-accessible Geographic Information System (GIS) user interface.

2. Accessing the Application

- a. The BSEE Sensor Application requires users to be signed in to the application before accessing any part of the program. To sign in to the BSEE Sensor Application, the user will need to enter an email address and password. Users who do not have an account will need to click the Register Now link below the sign in button.

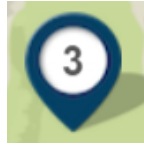
The screenshot shows the BSEE Sensor Application sign-in page. At the top is the BSEE logo with the text "Sensor Application" below it. Below the logo are two yellow input fields: the first contains the email address "test@test.com" and the second contains a masked password "*****". Below these fields is a dark blue "Sign In" button. To the right of the button is a link that says "New here? Register now!"

- b. The registration process requires an email address, user name, and password.
 - i. Passwords for the BSEE Sensor Application must be at least 8 characters long and must use 3 of the following 4 when creating password: upper case, lower case, number, special character (!, @, #, \$, etc.)

The screenshot shows the BSEE Sensor Application registration page. At the top is the BSEE logo with the text "Sensor Application" below it. Below the logo are four light gray input fields, each with an icon and a label: an envelope icon for "Email Address", a person icon for "User Name", a padlock icon for "Enter Password", and another padlock icon for "Confirm Password". Below these fields is a dark blue "Register" button. To the right of the button is a link that says "Already Have An Account? Sign In"

3. Common Terms

- a. Tag ID: This is a unique ID for LDGRIDSAT tags, and each UWID tag associated with an LDGRIDSAT tag will also have a unique ID. Administrators use these tag IDs to add LDGRIDSAT tags to the BSEE Sensor Application and distinguish unique IDs for detected UWID tags per LDGRIDSAT tag.
- b. Tag: A physical device used to identify, locate and track objects that it is attached to. LDGRIDSATs and UWIDs are types of tags.



- i. LDGRIDSAT Tags: An LDGRIDSAT tag is a GPS and satellite modem-enabled radio-frequency device that detects signals through guided waves generated from UWID tags and acts as a gateway to communicate UWID tag identification, time and sequence number information to the BSEE Sensor Application.
 - ii. UWID Tags: UWID tags are acoustic generating devices deployed beneath the ice for detection by the surface LDGRIDSAT tags.
- c. GRID Tag: A general technology category of which LDGRIDSAT tags are one type.

4. Startup Navigation

- a. Upon logging in to the application, a user will see a map similar to the image below with the following features:

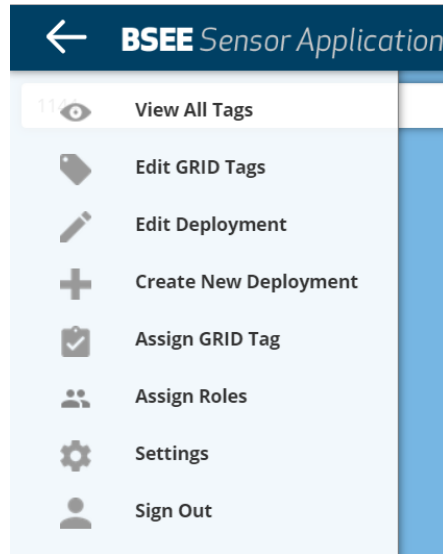


- i. User Name (#1)
 - i. The top right hand corner of the navigation bar will display the name of the current user logged into the application.
- ii. Notification (#2)
 - i. The BSEE Sensor Application will notify the user when LDGRIDSAT tags have been assigned to the user. Notifications will persist in the top navigation bar and will reset after the user views the All Tags page.
- iii. Search (#3)
 - i. The search box allows users to search the BSEE Sensor Application using longitude and latitude, places of interest, tag ID, or tag name
- iv. Map Navigation
 - i. A user can click and hold/drag to move the map.
- v. The map can be zoomed in or out using the buttons at the bottom left or the mouse scroll wheel.



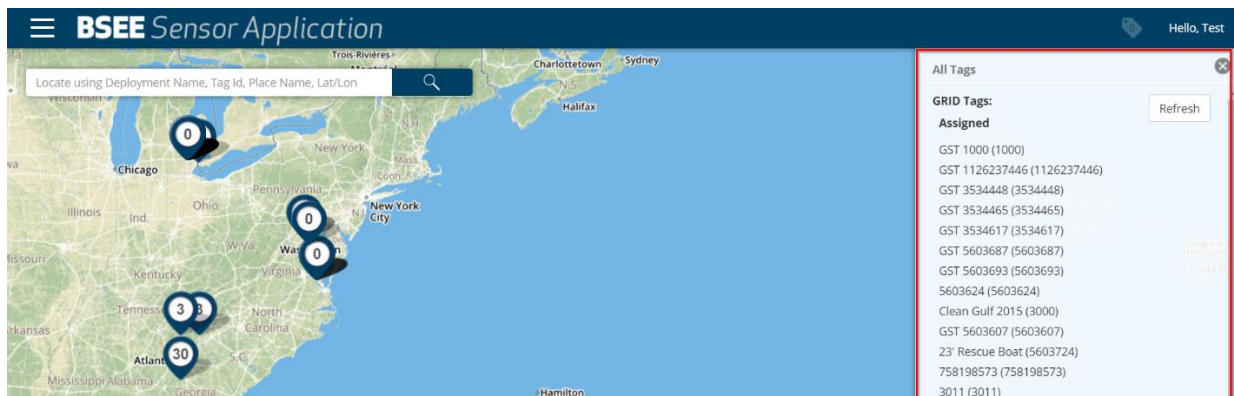
- vi. Main Menu (#4)
 - i. The main menu of the BSEE Sensor Application will be accessible using the menu icon (three horizontal lines). The user can access the following actions from the menu:
 - a. View All Tags

- b. Edit GRID Tags
- c. Edit Deployment
- d. Create New Deployment
- e. Assign GRID Tag
- f. Assign Roles
- g. Settings
- h. Sign Out



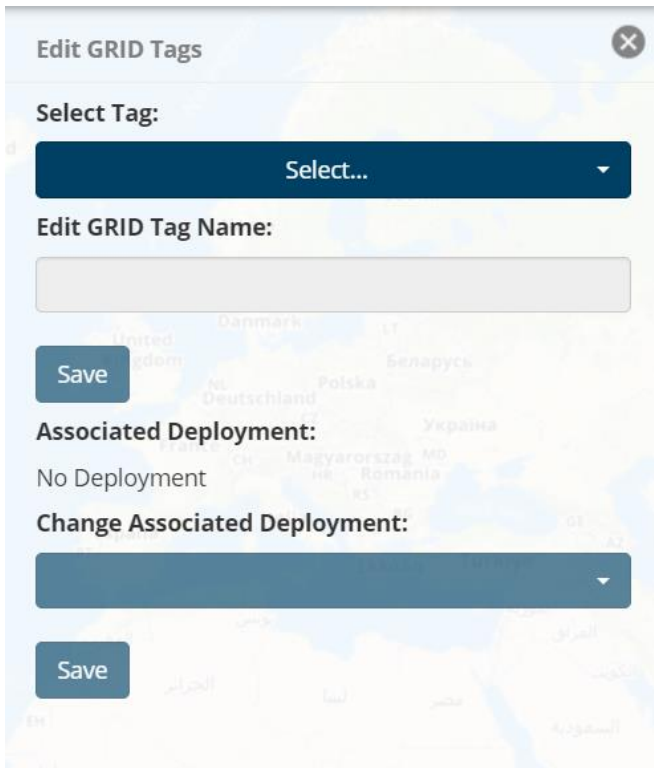
5. View All Tags

- a. This action allows the user to see all of the LDGRIDSAT tags assigned to him or her. Clicking View All Tags in the menu will open up a panel to the right with two distinct sections: Assigned Tags and Unassigned Tags.
 - i. Unassigned Tags: Any tags that have not been associated to a user. There will also be an indicator to show which of the previously unassigned LDGRIDSAT tags have been assigned to the user by an Administrator or Super User.

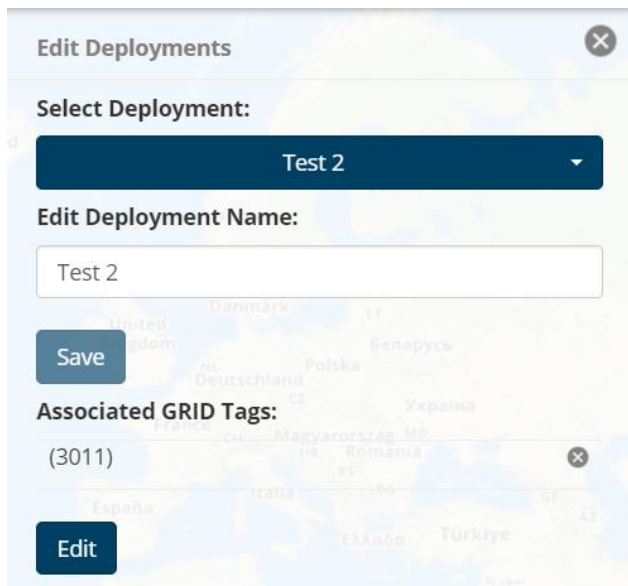


6. Edit GRID Tags

- a. Clicking this option in the Main Menu will open a panel to the right that will allow the user to edit the tag name and change the associated deployment.



7. Edit Deployment
 - a. Clicking this option from the Main Menu will allow the user to edit the deployment name and see which LDGRIDSAT tags are associated with a deployment.



8. Create New Deployment
 - a. Clicking this option on the Main Menu will open a popup window to begin creating a new deployment. The user must first name the deployment and click Create.

Create Deployment

Step One: Deployment Name

Name the deployment

Create

- b. After the user clicks Create, a second popup will appear asking the user to add tags to the deployment using the map or choosing from a list of tags.

Create Deployment

Step Two: Manage GRID Tags

How do you want to add/remove GRID Tags for this deployment?

Back View Map View List

- c. Clicking View Map will allow the user to select the tags from the map.

Update Deployment

Step Three: Manage GRID Tags - Map

Select the GRID Tags you would like to add to the deployment

Leaflet

Back Next

d. Clicking View List will bring up all tags in a checklist.

Update Deployment
Step Three: Manage GRID Tags - List

Select the GRID Tags you would like to add to the deployment

GRID Tags

Assigned

- GST 1000
- GST 3534465
- GST 5603693
- GST 5603607
- 3011
- GST 5603655
- 3009
- 1144
- 276100
- 307000
- 205980
- 255
- 5620292
- GST 1126237446
- GST 3534617
- 5603624
- 23' Rescue Boat
- 759510
- 5603626
- 3010
- 273080
- 3001
- 301020
- 206980
- 14
- GST 3534448
- GST 5603687
- Clean Gulf 2015
- 758198573

Unassigned

- 0
- 3012
- 276090
- 18587840
- 277080
- 15
- 1001

Back Next

e. Once the user has selected tags to associate with a deployment, clicking Next will display a popup to verify the new deployment. The user has the option to go back and adjust the deployment or click Finished to create the new deployment.

Update Deployment
Step Four: Review Deployment

Review the deployment information below

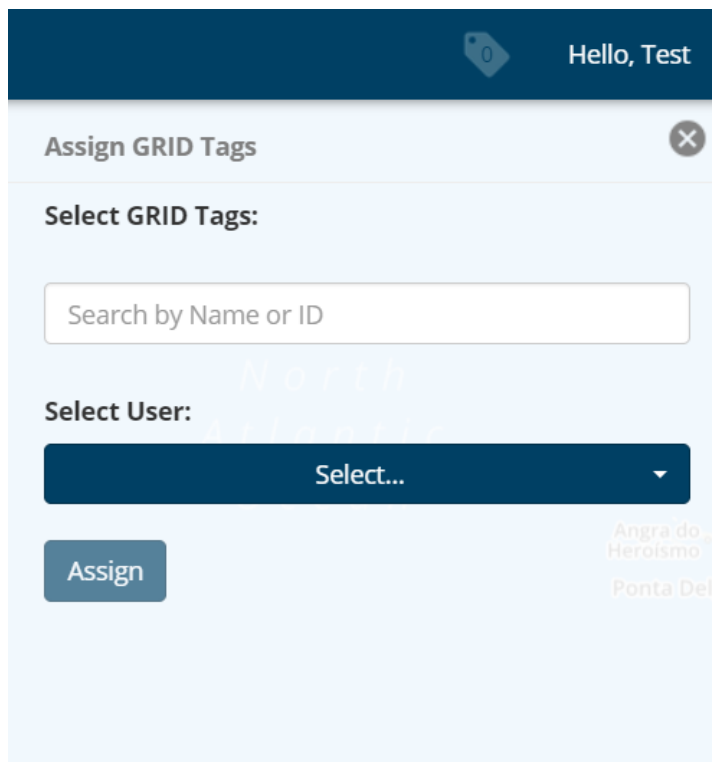
Name
Test

GRID Tags
✕ 273080 (273080)

Back Finished

9. Assign GRID Tag

- a. Clicking this option from the Main Menu will open a panel to the right where LDGRIDSAT tags can be assigned to users.

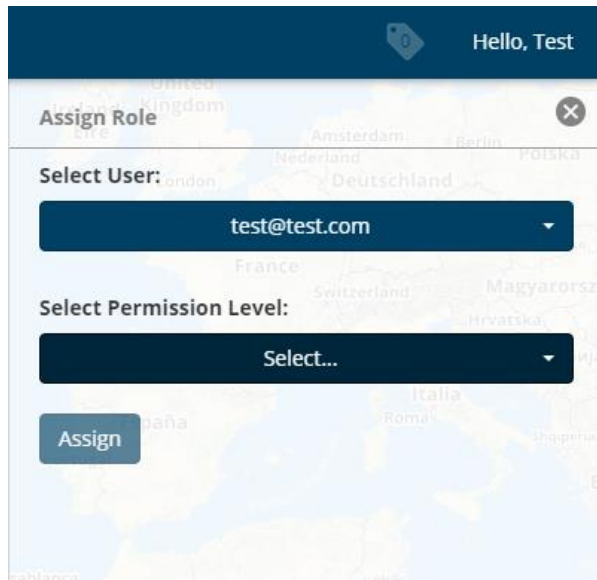


- i. Administrators and Super Users can assign LDGRIDSAT tags to users. Once assigned, a notification will be displayed to the user.



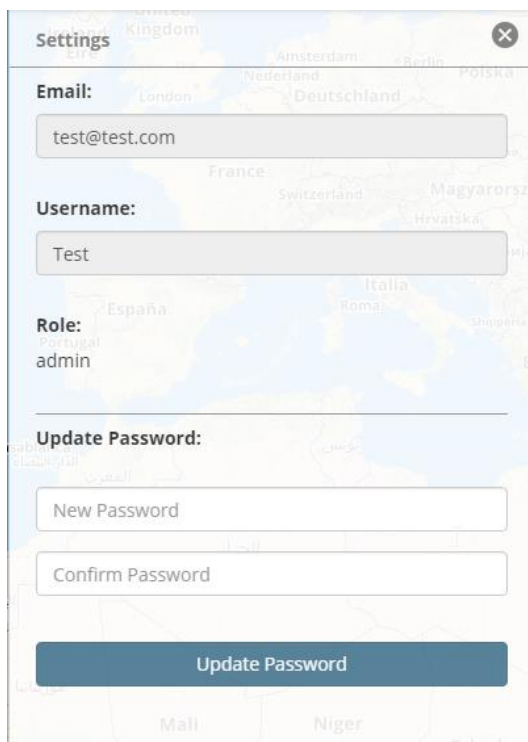
10. Assign Role

- a. There are three roles with three distinct permission levels within the BSEE Sensor Application. The three roles are Administrator, Super User, and Regular User:
 - i. Administrator: the highest user setting in the BSEE Sensor Application. An administrator can see all Tags, add LDGRIDSAT Tags to the system, change a user's role, and assign LDGRIDSAT Tags to users.
 - ii. Super User: the middle user setting in the BSEE Sensor Application. A Super User can see all Tags and assign LDGRIDSAT Tags to users. The only operations a Super User cannot perform is adding Tags to the system and modifying a user's role.
 - iii. Regular User: the lowest user setting in the BSEE Sensor Application. A Regular User can only see the Tags an Administrator or Super User has assigned to the user.



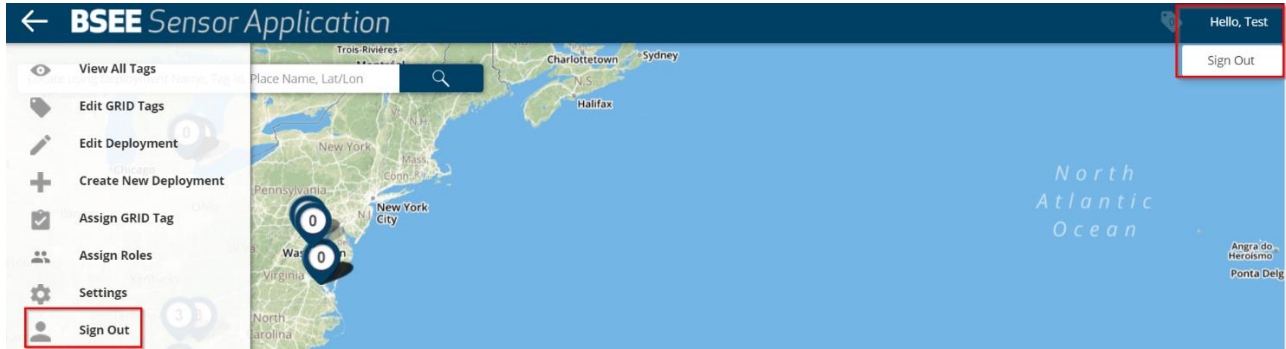
11. Settings

- a. Clicking on Settings in the Main Menu will display a panel to the right containing the following: Email, Username, Update Password and Role.
 - i. Update Password: Type a new password and re-enter the password to confirm that password. When you are done, click the Update Password button.
 - a. Passwords for the BSEE Sensor Application must be at least 8 characters long and must use 3 of the following 4 when creating password: upper case, lower case, number, special character (!, @, #, \$, etc.).



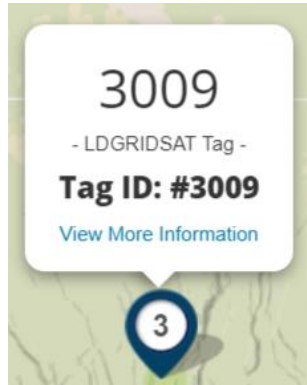
12. Sign Out

- a. There are two ways to sign out of the application.
 - i. Users can click on the Sign Out link at the bottom of the main menu.
 - ii. Users can also sign out by clicking their Username in the upper right corner of the navigation bar.

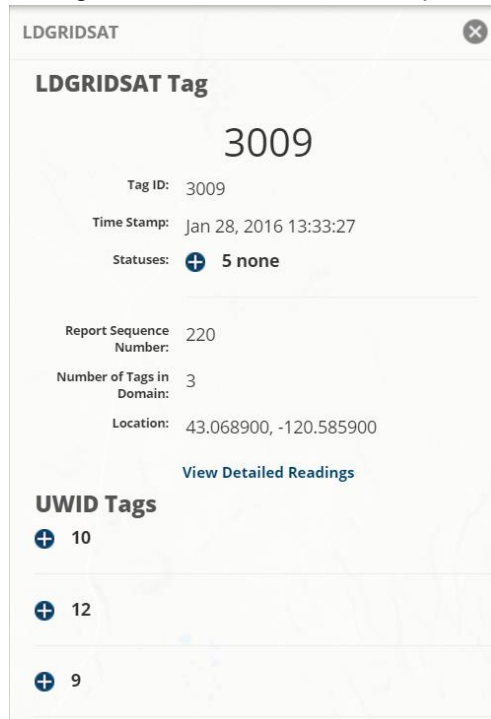


13. Accessing Tag Information

- a. Clicking on an LDGRIDSAT tag will display a popup with the Tag ID:



- b. Clicking on View More Information opens a panel to the right of the screen:

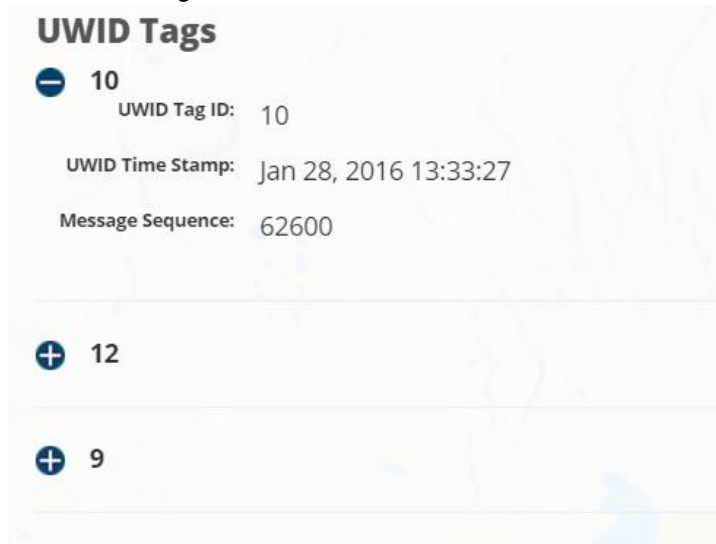


Definitions for terms found in the above panel:

1. Time Stamp:- The Time Stamp is the time when the LDGRIDSAT tag last collected or transmitted data.
 2. Report Sequence Number: Number of consecutive reports transmitted to the BSEE Sensor Application from a LDGRIDSAT tag since powering on.
 3. Number of Tags in Domain: The number of UWID tags associated with a given LDGRIDSAT tag.
 4. Location: The latitude and longitude location of the tag.
- b. Status: Clicking the plus sign next to Statuses will display the current status message. Messages displayed include: Status OK, Battery Low, GPS Fault, No GPS Fix, RF Module Fault, and Reserved.



- c. UWID Tags: Clicking the plus sign in the panel next to a UWID tag ID will expand the details for that tag.



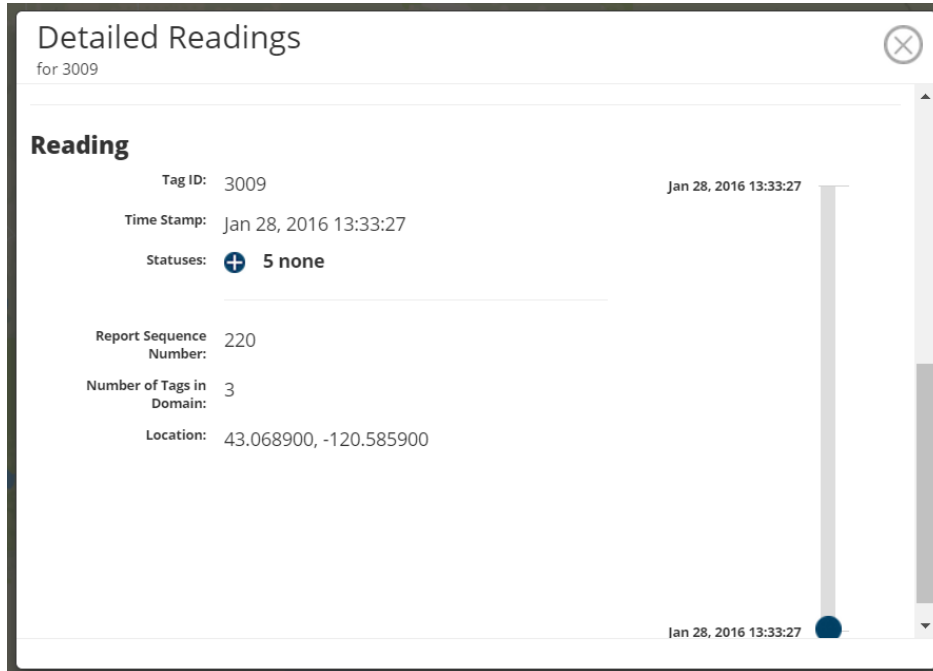
- i. Definitions for terms in UWID Tags details

1. UWID Tag ID: This is the ID number associated with the UWID tag.
2. UWID Time Stamp: The time when the LDGRIDSAT last detected the UWID signal.
3. Message Sequence: This is the number of consecutively detected signals by the LDGRIDSAT tag from a UWID tag since the LDGRIDSAT tag was powered on.

- d. Detailed Readings

- i. Clicking on View Detailed Readings in the View More Information Panel will open a popup window. Detailed Readings contains two categories: Reading and Location.

1. The Reading section shows the following readings: Tag ID, Time Stamp, Statuses, Report Sequence Number, Number of Tags in Domain, and Location. There is a scrub slider that allows the user to see all of the aforementioned readings at different times over the life of the LDGRIDSAT tags.



2. The Location section shows the position (visually and numerically) over time. There is a scrub slider that allows the user to select a particular point in time and thus the position of the LDGRIDSAT tag.

